

# 博士學位論文

多重免疫染色を用いた非小細胞肺癌における免疫チ  
ェックポイント阻害薬の初期耐性と獲得耐性機序の  
検討

近畿大学大学院  
医学研究科医学系専攻  
磯本晃佑

# Doctoral Dissertation

## **Mechanisms of primary and acquired resistance to immune checkpoint inhibitors in advanced non–small cell lung cancer: a multiplex immunohistochemistry– based single-cell analysis**

November 2022


Major in Medical Sciences  
Kindai University Graduate School of Medical Sciences

**Kohsuke Isomoto**

同意書


2022年11月7日

近畿大学大学院  
医学研究科長 殿


共著者 林秀敏 


共著者 米阪仁敬 


共著者 田中董 

共著者 岩朝嘉 

共著者 武田真幸 

共著者 原谷浩司 

共著者 川上尚人 

共著者 幕谷悠介 

共著者 \_\_\_\_\_ 

共著者 \_\_\_\_\_ 

論文題目

Mechanisms of primary and acquired resistance to immune checkpoint inhibitors in advanced non-small cell lung cancer: a multiplex immunohistochemistry-based single-cell analysis

下記の博士論文提出者が、標記論文を貴学医学博士の学位論文（主論文）として使用することに同意いたします。  
また、標記論文を再び学位論文として使用しないことを誓約いたします。

記

1. 博士論文提出者氏名

磯本晃佑

2. 専攻分野 医学系

腫瘍病態制御学

同意書

2022年10月25日

近畿大学大学院  
医学研究科長 殿

共著者 辻川敬裕 (印) 共著者 \_\_\_\_\_ (印)  
共著者 \_\_\_\_\_ (印) 共著者 \_\_\_\_\_ (印)  
共著者 \_\_\_\_\_ (印) 共著者 \_\_\_\_\_ (印)  
共著者 \_\_\_\_\_ (印) 共著者 \_\_\_\_\_ (印)  
共著者 \_\_\_\_\_ (印) 共著者 \_\_\_\_\_ (印)

論文題目

Mechanisms of primary and acquired resistance to immune checkpoint inhibitors in advanced non-small cell lung cancer: a multiplex immunohistochemistry-based single-cell analysis

下記の博士論文提出者が、標記論文を貴学医学博士の学位論文（主論文）として使用することに同意いたします。

また、標記論文を再び学位論文として使用しないことを誓約いたします。


記

1. 博士論文提出者氏名 磯本晃佑  
2. 専攻分野 医学系 腫瘍病態制御学

同意書

2022 年 11 月 7 日

近畿大学大学院  
医学研究科長 殿

共著者	<u>伊藤 彰彦</u>		共著者	_____	印
共著者	_____	印	共著者	_____	印
共著者	_____	印	共著者	_____	印
共著者	_____	印	共著者	_____	印
共著者	_____	印	共著者	_____	印

論文題目

Mechanisms of primary and acquired resistance to immune checkpoint inhibitors in advanced non-small cell lung cancer: a multiplex immunohistochemistry-based single-cell analysis

下記の博士論文提出者が、標記論文を貴学医学博士の学位論文（主論文）として使用することに同意いたします。

また、標記論文を再び学位論文として使用しないことを誓約いたします。

記

- |              |         |
|--------------|---------|
| 1. 博士論文提出者氏名 | 磯本晃佑    |
| 2. 専攻分野 医学系  | 腫瘍病態制御学 |

同意書

2022年11月7日

近畿大学大学院  
医学研究科長 殿

共著者	<u>磯本晃佑</u> 	共著者	_____ 
共著者	_____ 	共著者	_____ 
共著者	_____ 	共著者	_____ 
共著者	_____ 	共著者	_____ 
共著者	_____ 	共著者	_____ 

論文題目

Mechanisms of primary and acquired resistance to immune checkpoint inhibitors in advanced non-small cell lung cancer: a multiplex immunohistochemistry-based single-cell analysis

下記の博士論文提出者が、標記論文を貴学医学博士の学位論文（主論文）として使用することに同意いたします。  
また、標記論文を再び学位論文として使用しないことを誓約いたします。


記

- |              |         |
|--------------|---------|
| 1. 博士論文提出者氏名 | 磯本晃佑    |
| 2. 専攻分野 医学系  | 腫瘍病態制御学 |

同意書

2022 年 11 月 7 日

近畿大学大学院  
医学研究科長 殿

共著者 中川和彦 

共著者 \_\_\_\_\_ (印)

共著者 \_\_\_\_\_ (印)

共著者 \_\_\_\_\_ (印)

共著者 \_\_\_\_\_ (印)

共著者 \_\_\_\_\_ (印)

共著者 \_\_\_\_\_ (印)

共著者 \_\_\_\_\_ (印)

共著者 \_\_\_\_\_ (印)

共著者 \_\_\_\_\_ (印)

論文題目

Mechanisms of primary and acquired resistance to immune checkpoint inhibitors in advanced non-small cell lung cancer: a multiplex immunohistochemistry-based single-cell analysis

下記の博士論文提出者が、標記論文を貴学医学博士の学位論文（主論文）として使用することに同意いたします。

また、標記論文を再び学位論文として使用しないことを誓約いたします。

記

1. 博士論文提出者氏名

磯本晃佑

2. 専攻分野 医学系

腫瘍病態制御学

# **Mechanisms of primary and acquired resistance to immune checkpoint inhibitors in advanced non–small cell lung cancer: a multiplex immunohistochemistry–based single-cell analysis**

Kohsuke Isomoto<sup>1</sup>, Koji Haratani<sup>1,\*</sup>, Takahiro Tsujikawa<sup>2</sup>, Yusuke Makutani<sup>3</sup>, Hisato Kawakami<sup>1</sup>, Masayuki Takeda<sup>1</sup>, Kimio Yonesaka<sup>1</sup>, Kaoru Tanaka<sup>1</sup>, Tsutomu Iwasa<sup>1</sup>, Hidetoshi Hayashi<sup>1</sup>, Akihiko Ito<sup>4</sup>, Kazuto Nishio<sup>5</sup>, Kazuhiko Nakagawa<sup>1</sup>

<sup>1</sup>Department of Medical Oncology, Kindai University Faculty of Medicine, Osaka-Sayama, Japan

<sup>2</sup>Department of Otolaryngology–Head & Neck Surgery, Kyoto Prefectural University of Medicine, Kyoto, Japan

<sup>3</sup>Department of Surgery, Kindai University Faculty of Medicine, Osaka-Sayama, Japan <sup>4</sup>Department of Pathology, Kindai University Faculty of Medicine, Osaka-Sayama, Japan <sup>5</sup>Department of Genome Biology, Kindai University Faculty of Medicine, Osaka-Sayama, Japan

\*Corresponding author at: Department of Medical Oncology, Kindai University Faculty of Medicine, 377-2 Ohno-higashi, Osaka-Sayama, Osaka 589-8511, Japan. Tel.: +81-72-366-0221. Fax: +81-72-360-5000. Email: haratani\_k@med.kindai.ac.jp



## **ABSTRACT**

*Objective:* Immune checkpoint inhibitors (ICIs) have become a key therapeutic modality for advanced non–small cell lung cancer (NSCLC), but most patients experience primary or acquired resistance to these drugs. We here explored the mechanisms underlying both types of ICI resistance by analysis of the tumor immune microenvironment (TME).

*Materials and methods:* Four patients who experienced a long-term response to ICI treatment (progression-free survival [PFS] of  $\geq 12$  months) followed by disease progression, after which a rebiopsy was immediately performed (cohort-A), as well as four patients who experienced early tumor progression during ICI treatment (PFS of  $< 9$  weeks, cohort-B) were enrolled in this retrospective study. The pretreatment TME was evaluated by 16- or 17-color multiplex immunohistochemistry (mIHC)–based spatial profiling at the single-cell level for both cohorts. In cohort-A, changes in the TME after disease progression during ICI treatment were also investigated by mIHC analysis and transcriptomic analysis.

*Results:* Pretreatment tumor tissue from cohort-B manifested poor infiltration of tumor-reactive CD8<sup>+</sup> T cells characterized by CD39 and CD103 expression or by programmed cell death–1 expression, implicating insufficient recognition of tumor cells by CD8<sup>+</sup> T cells as a mechanism of primary ICI resistance. Analysis of the paired tumor specimens from cohort-A revealed various changes in the TME associated with acquired ICI resistance, including substantial infiltration of myeloid-derived suppressor cells and M2-type tumor-associated macrophages without a marked decline in the number of tumor-reactive CD8<sup>+</sup> T cells; a decrease in the number of tumor-reactive CD8<sup>+</sup> T cells; and an apparent decrease in neoantigen presentation by tumor cells.

*Conclusion:* The presence of intratumoral tumor-reactive CD8<sup>+</sup> T cells may be a prerequisite for a long-term response to ICI treatment in advanced NSCLC, but it is not sufficient for cancer cell eradication. Various TME profiles are associated with acquired ICI resistance, suggesting that patient-specific strategies to overcome such resistance may be necessary.

## **Keywords**

Non-small cell lung cancer, Immune checkpoint inhibitor, Primary resistance, Acquired resistance,  
Tumor immune microenvironment, Multiplex immunohistochemistry

## **1. Introduction**

The advent of immune checkpoint inhibitors (ICIs) has brought about a paradigm shift in the treatment of non–small cell lung cancer (NSCLC) [1-6]. Despite this clinical success, however, lung cancer remains the leading cause of cancer-related deaths worldwide, in part because most patients have tumors that are resistant to ICI treatment [7]. There are two main clinical scenarios for ICI resistance that are reflected by the time course of its development [8]. Most patients manifest primary resistance, which is characterized by early tumor progression without durable disease control being achieved by ICI treatment. Primary resistance has been well studied, with poor infiltration of CD8<sup>+</sup> T cells into the tumor before treatment, a low expression level of programmed cell death–ligand 1 (PD-L1) on tumor cells, and a low tumor mutation burden or neoantigen load in tumor cells having been suggested as underlying mechanisms [9-11]. On the other hand, other patients experience acquired resistance, which is characterized by development of disease progression after long-term tumor control (up to years) by ICI treatment. The mechanisms of acquired resistance remain largely uncharacterized as a result of the difficulty of accessing tumor tissue after its development [12]. The clinical outcome after failure of ICI treatment is poor, with attempts to develop new immunotherapy regimens for such patients not having been successful to date. Detailed elucidation of ICI resistance mechanisms is thus important for further optimization of treatment strategies for NSCLC.

Accumulating evidence has implicated the tumor immune microenvironment (TME) as a key determinant of tumor fate including the invasion and metastasis of cancer cells [13-15]. In addition to cancer cells, the TME encompasses immune cells—including T and B lymphocytes, tumor-associated macrophages (TAMs), natural killer (NK) cells, myeloid-derived suppressor cells (MDSCs), and dendritic cells (DCs)—as well as nonimmune cells such as fibroblasts and endothelial cells, all of which interact at the cellular or molecular level in a complex manner [16]. However, how these various TME components are related to ICI resistance mechanisms remains poorly defined. In particular, further investigation of TME profiles that contribute to acquired resistance to ICIs is a clinical priority [8].

We have now conducted a retrospective biomarker analysis to evaluate the mechanisms of resistance to programmed cell death-1 (PD-1) and PD-L1 inhibitor treatment in advanced NSCLC with the use of multiplex immunohistochemistry (mIHC). We collected both pretreatment and posttreatment tumor tissue samples for mIHC analysis from four patients who experienced acquired resistance after long-term tumor control by PD-1/PD-L1 inhibitor treatment. Gene expression profiles were also compared between before and after resistance development. In addition, we collected pretreatment tumor tissue for mIHC analysis from another four patients who experienced rapid disease progression after the onset of PD-1/PD-L1 inhibitor therapy. Simultaneous evaluation of 16 or 17 marker proteins by mIHC allowed quantitative spatial profiling of various cell lineages in the intratumoral area at the single-cell level. Our findings identified TME profiles associated with primary or acquired resistance to PD-1/PD-L1 blockade therapy in advanced NSCLC.

## **2. Materials and Methods**

### *2.1. Patients*

We consecutively reviewed the medical records of all patients with advanced or recurrent NSCLC treated with PD-1 or PD-L1 inhibitor monotherapy at Kindai University Hospital between December 2015 and September 2021. Among these patients, those with pretreatment archival tumor tissue specimens available were selected for potential inclusion in the study. Individuals were excluded if their tumors tested positive for an epidermal growth factor receptor (EGFR) gene mutation or anaplastic lymphoma kinase (ALK) fusion gene, or if they had an Eastern Cooperative Oncology Group performance status of  $\geq 2$ . Patients were also excluded if their tumor tissue specimens were obtained by transbronchial needle aspiration or were cell block specimens, given that these types of specimen are not appropriate for spatial TME analysis. In addition, 60 patients were not considered for our mIHC analysis because the amount of tumor tissue available was too small. From this review, we identified 67 individuals who were potentially evaluable. Patients were selected for cohort-A if they also had tumor tissue available that was obtained immediately after they acquired resistance to the PD-1/PD-L1 inhibitor treatment, with acquired resistance being defined as disease progression

after long-term tumor control (progression-free survival [PFS] of  $\geq 12$  months) by the treatment. Patients were selected for cohort-B if they manifested primary resistance to PD-1/PD-L1 inhibitor treatment, with primary resistance being defined as a PFS of  $< 9$  weeks and a best response of progressive disease. The details of patient recruitment are shown in **Figure 1**. This retrospective study was performed according to the Declaration of Helsinki and protocols approved by the institutional review board of Kindai University Hospital.

## *2.2. Data collection*

Data regarding clinicopathologic features and treatment history were extracted from medical records and were updated as of 1 June 2022. Responses were assessed according to Response Evaluation Criteria in Solid Tumors version 1.1. PFS was measured from treatment initiation to clinical or radiographic progression or death from any cause.

## *2.3. mIHC staining protocol*

We performed mIHC staining as described previously [17-19]. In brief, for identification of the nucleus of each cell, sections of formalin-fixed paraffin embedded (FFPE) tissue (thickness, 4  $\mu\text{m}$ ) were depleted of paraffin, stained with hematoxylin (S3301, Dako), and subjected to whole-tissue scanning with a NanoZoomer instrument (Hamamatsu Photonics) at 20 $\times$  magnification. Endogenous peroxidase activity was then blocked by incubation of the sections with 0.6% hydrogen peroxide in phosphate-buffered saline for 15 min. Antigen retrieval was performed by microwave irradiation (to achieve a temperature of 95 $^{\circ}\text{C}$  for 15 min) in citrate buffer at pH 6.0 (RM102-C, LSI Medience). The slides were then exposed to 5.0% goat serum and 2.5% bovine serum albumin in phosphate-buffered saline to block nonspecific sites before sequential incubation with primary antibodies; anti-mouse, anti-rabbit, anti-rat, or anti-goat Histofine Simple Stain MAX PO horseradish peroxidase-conjugated polymer (Nichirei Biosciences); and the alcohol-soluble peroxidase substrate 3-aminoethyl carbazole in the order shown in **Supplementary Table S1**. Goat serum was removed from the blocking buffer before exposure of the sections to anti-goat secondary antibodies. Stained

sections were scanned with the NanoZoomer instrument at 20× magnification. Chromogenic destaining and antibody stripping were performed between the sequential staining steps.

#### *2.4. Digital analysis*

Representative fields (0.50 to 3.55 mm<sup>2</sup>) were randomly selected from intratumoral areas with the use of Aperio ImageScope version 12 software (Leica Biosystems). The presence of tumor cells in these areas was confirmed by a board-certified pathologist. Each region of interest was further categorized into a tumor cell nest area and a non-tumor cell area with the use of a mathematical morphological approach performed with the Tissue Segmentation platform developed in our previous study [20]. Between one and four fields of view were evaluated depending on the size of the tumor (average of 2.0 fields of view). Image processing and subsequent computational analysis were performed with ImageJ/Fiji version 1.51 (National Institutes of Health), CellProfiler version 2.2.0 (Broad Institute), Aperio ImageScope, and FCS Express 7 Image Cytometry version 7.04.0020 (De Novo Software) [17-19]. In brief, iteratively digitized images were accurately coregistered with the use of in-house software (SCREEN Holdings Co. Ltd.) that calculates the coordinates of each image relative to a reference one (any one of the images). With the use of these coordinates, a set of noncompressed TIFF images for each region of interest was extracted. Single-cell segmentation and quantification of staining intensity were then performed with an ImageJ/Fiji and CellProfiler pipeline. Quantitative evaluation of staining intensity for single cells was performed with FCS Express 7 Image Cytometry. Fluorescence-minus-one controls were used to determine true positive cells. The final value for each cell number was calculated as the average of values from the multiple fields of view. Visualization of each staining was performed by pseudocoloring with ImageJ/Fiji and Aperio ImageScope.

#### *2.5. NanoString immune-related gene expression panel analysis*

Isolation of RNA from FFPE tumor tissue and gene expression analysis were performed as described previously [21]. In brief, tumor tissue was microdissected to avoid contamination from nontumor

tissue before extraction of intratumoral RNA with the use of an AllPrep DNA/RNA FFPE Kit (Qiagen). The quality of the isolated RNA was assessed with a NanoDrop system (Thermo Fisher Scientific) and an Agilent 2100 Bioanalyzer (Agilent Technologies) before analysis with the nCounter platform and a PanCancer IO 360 Panel comprising 750 immune-related genes and 20 housekeeping genes (NanoString Technologies). Sample-to-sample normalization of gene expression was performed on the basis of data for the 20 housekeeping genes with the use of nSolver Analysis Software 4.0 and nCounter Advanced Analysis 2.0 (NanoString Technologies). Samples with aberrant normalized expression values (normalization factor of >10 obtained with nSolver Analysis Software 4.0) were excluded, as recommended by the manufacturer. A total of seven RNA samples remained for further analysis. Of the 750 immune-related genes, we filtered out 26 genes for which >90% of samples had expression values below the minimum threshold. The normalized gene expression data were log<sub>2</sub>-transformed before calculation of the Z score. Signature scores for gene set analysis were calculated with nCounter Advanced Analysis 2.0.

### *2.6. Statistical analysis*

The Mann-Whitney U test was applied for comparison of continuous variables. Paired data were compared with the Wilcoxon signed rank test. All *P* values were based on a two-sided hypothesis. Statistical analysis was performed with GraphPad Prism software version 8.4.3.

## **3. Results**

### *3.1. Patient characteristics*

Eight patients were enrolled in the study. Patients with a PFS on ICI treatment of  $\geq 12$  months or <9 weeks were assigned to cohort-A ( $n = 4$ ) and cohort-B ( $n = 4$ ), respectively. All patients in cohort-A underwent rebiopsy at the time of disease progression during ICI treatment (**Fig. 1**). Patient characteristics were similar between cohort-A and cohort-B (**Table 1**). The median age for all patients was 71 years. The distribution of PD-L1 tumor proportion score (TPS) was well balanced between the two cohorts. The median PFS for ICI treatment of patients in cohort-A and cohort-B

was 618.5 and 42 days, respectively.

### *3.2. Association of primary resistance to PD-1/PD-L1 blockade therapy with poor infiltration of CD8<sup>+</sup> T cells with neoantigen-reactive phenotypes into the tumor nest*

All four patients in cohort-A experienced long-term tumor regression with PD-1/PD-L1 inhibitor treatment that persisted for >17 months, in contrast to the rapid disease progression after the start of such treatment apparent in cohort-B. We hypothesized that this marked difference in initial response to PD-1/PD-L1 inhibitors was attributable to a difference in the pretreatment TME. To investigate this hypothesis, we performed single-cell spatial profiling of immune cells infiltrating the tumor nest by mIHC analysis with our novel digital pathology platform [17]. We first evaluated intratumoral antitumor lymphocytes including T cells and NK cells, as well as regulatory T cells (Tregs). Each cell lineage was defined as shown in **Figure 2A** and **Supplementary Table S2**. Infiltration of T cells and CD8<sup>+</sup> T cells into the tumor sites was more pronounced in cohort-A than in cohort-B, although infiltration of pan-leukocytes (CD45<sup>+</sup> cells) including non-T cells was similar in the two cohorts (**Fig. 2B**). Other antitumor lymphocytes such as T helper 1 and NK cells did not show preferential infiltration into the tumors of the long-term responders. In addition, the number of Tregs did not differ substantially between the two cohorts. These data suggested that the presence of CD8<sup>+</sup> T cells in the tumor nest before treatment might contribute to tumor control by PD-1/PD-L1 inhibitors.

We next investigated the detailed phenotypes of the antitumor CD8<sup>+</sup> T cells. Previous studies have suggested that the presence of CD8<sup>+</sup> T cells expressing the conventional activated T cell markers granzyme B, Ki-67, and T-box expressed in T cells (T-bet) is associated with a favorable survival outcome in other types of cancer [22-24]. However, no difference in the numbers of these CD8<sup>+</sup> T cell subsets was detected between the two cohorts of the present study (**Supplementary Fig. S1A**). Recent studies based on single-cell RNA-sequencing analysis have shown that neoantigen-specific T cells can be identified by CD39 or CD103 expression as tissue-resident memory (Trm)-like T cells, whose presence in the TME has been associated with an improved response to ICI treatment [25, 26]. Indeed, we found that the number of Trm-like (CD39<sup>+</sup>CD103<sup>+</sup>) CD8<sup>+</sup> T cells in



the tumor nest was significantly greater in cohort-A than in cohort-B (**Fig. 2C** and **D**). In addition, PD-1 has been suggested as a marker of clonally expanded tumor-specific T cells, with its expression on CD8<sup>+</sup> T cells thus being expected to be associated with a better efficacy of ICI treatment. PD-1 positivity among tumor-infiltrating CD8<sup>+</sup> T cells was higher for cohort-A than for cohort-B (**Fig. 2C**). On the other hand, PD-1 is also a co-inhibitory molecule, and we examined other co-inhibitory molecules such as lymphocyte activation gene-3 (LAG-3), T cell immunoglobulin and mucin domain containing-3 (TIM-3), and T cell immunoreceptor with immunoglobulin and ITIM domains (TIGIT). The expression of these co-inhibitory molecules in CD8<sup>+</sup> T cells did not differ substantially between the two cohorts (**Supplementary Fig. S1B**). Expression of CD39 or PD-1 on Tregs also did not differ between the two cohorts (**Supplementary Fig. S1C**).

Overall, these data suggested that primary resistance of metastatic NSCLC to PD-1/PD-L1 blockade therapy might be due to the presence of an insufficient number of tumor-infiltrating CD8<sup>+</sup> T cells—in particular, of neoantigen-reactive T cell subsets—before treatment onset. Immunosuppressive mechanisms such as those mediated by Tregs or co-inhibitory molecules in T cells did not appear to contribute to such primary resistance.

### *3.3. Lack of a clear association between immune-related myeloid cells in the tumor nest or immune-related stromal cells and primary resistance to PD-1/PD-L1 blockade therapy*

In addition to lymphocytes, other immune cell subsets and stromal cells are considered important components of the TME [27]. In particular, M2-type TAMs, MDSCs, and cancer-associated fibroblasts (CAFs) have been suggested to play an immunosuppressive role by preclinical studies [28, 29]. We therefore next evaluated the relation of these putative immunosuppressive cells to the initial tumor response to PD-1/PD-L1 inhibitor treatment. We also examined other immunogenic myeloid cells such as M1-TAMs as well as DCs and several checkpoint markers including CD73 and B7-H3 expressed on tumor cells. In addition, we assessed tertiary lymphoid structures (TLSs) by analyzing follicular DCs (FDCs) expressing peripheral lymph node addressin (PNAd). These various cell lineages were defined as shown in **Figure 3A** and **Supplementary Table S2**.

The number of pan-myeloid (CD45<sup>+</sup>CD3<sup>-</sup>CD20<sup>-</sup>) cells in the tumor nest was similar between the two cohorts (**Fig. 3B**). Pan-TAMs, M1-TAMs, and M2-TAMs were also not associated with the initial response to ICI treatment (**Fig. 3B**). The numbers of MDSCs and of the polymorphonuclear (PMN)-MDSC subset (CD66b<sup>+</sup> MDSCs) were found to be increased in two nonresponders in cohort-B, but the overall differences between the two cohorts were not apparent (**Fig. 3C**). Examination of professional antigen presenting cells (APCs) in the tumor nest also revealed that intratumoral infiltration of DCs did not differ between the two cohorts, regardless of the APC markers, including CD80 and DC-LAMP (lysosome-associated membrane protein), examined (**Fig. 3D**).

Stromal components implicated as determinants of ICI treatment efficacy were also examined in the two cohorts. We defined CAFs as fibroblast activation protein (FAP)-positive stromal cells, but the number of these cells was not associated with the initial response to ICI treatment (**Supplementary Fig. S2A**). FDCs, which are a main component of TLSs, were detected as CD45<sup>-</sup>PanCK<sup>-</sup>PNAd<sup>+</sup> cells; however, none of the 12 tumors from the 8 study patients showed a solid TLS characterized by accumulated T cells and B cells together with FDCs. These non-TLS-related FDCs were not associated with the initial ICI response (**Supplementary Fig. S2B**).

Previous studies have implicated CD73 and B7-H3 as potential resistance markers for ICI treatment [30, 31], and tumor cells were found to express these molecules at the cell surface in our cohorts (**Supplementary Fig. S2C**). However, the proportion of tumor cells expressing these molecules did not differ between the two cohorts (**Fig. 3E**).

#### *3.4. Immune profiles associated with acquired resistance to PD-1/PD-L1 inhibition*

In cohort-A, all four patients also had tumor tissue samples that were obtained immediately after the acquisition of resistance to PD-1/PD-L1 inhibition, and which were also subjected to analysis with our mIHC platform. We therefore investigated changes in immune profiles between pretreatment and postresistance tumor tissue. We detected no consistent changes in the TME between before and after the development of ICI resistance for these four patients (**Fig. 4A and B**). However, some unique

alterations in the immune profile of each patient were apparent that might have contributed to the acquired resistance.

Patient 1 was a current smoker with adenocarcinoma, the PD-L1 TPS for which was <1%. This patient experienced disease progression during nivolumab treatment as a second-line therapy, with a PFS of 19.8 months. The histological type of the resistant tumor was also adenocarcinoma. Unexpectedly, the CD8<sup>+</sup> tumor-infiltrating lymphocyte (TIL) density was found to be markedly increased after the development of resistance (from 106.4 to 470.8/mm<sup>2</sup>) (**Fig. 4A** and **C**). The proportions of these infiltrating CD8<sup>+</sup> T cells positive for a Trm-like phenotype or for PD-1 remained essentially unchanged (**Fig. 4A**), suggesting that these cells still recognized tumor cells as their immune target. Of interest, however, the numbers of MDSCs, PMN-MDSCs, and M2-TAMs were also greatly increased after acquisition of resistance (from 12.8 to 261.6/mm<sup>2</sup>, from 0.4 to 27.9/mm<sup>2</sup>, and from 2.9 to 182.5/mm<sup>2</sup>, respectively) (**Fig. 4B** and **C**). This postresistance MDSC density was even greater than that of pretreatment tissue from any of the nonresponders in cohort-B (**Fig. 3C**). In addition, the proportion of tumor cells expressing CD73 was increased after resistance development (from 6.4% to 61.3%) (**Fig. 4B**). Production of the immunosuppressive molecule adenosine by CD73 expressed on tumor cells was previously shown to recruit MDSCs and M2-TAMs into tumors and thereby to attenuate antitumor immunity [32, 33], suggesting that such a mechanism might have contributed to acquired resistance in this patient.

Patient 2 was a never-smoker with adenocarcinoma, the PD-L1 TPS for which was 10%. This patient received nivolumab as a third-line treatment and experienced a PFS of 25.4 months. The histological type of the resistant tumor was also adenocarcinoma. The CD8<sup>+</sup> TIL density was also increased after the development of ICI resistance in this patient (from 72.9 to 270.1/mm<sup>2</sup>) (**Fig. 4A**). However, positivity for the tumor-reactive phenotypes of CD8<sup>+</sup> TILs declined (Trm-like, from 95.4% to 65.7%; PD-1<sup>+</sup>, from 38.6% to 27.1%) (**Fig. 4A**).

Patient 3 was a former smoker with squamous cell carcinoma, the PD-L1 TPS for which was not evaluated. Sequencing analysis of posttreatment tumor tissue was performed in the clinic with the FoundationOne CDx test (Foundation Medicine) and revealed the G12C mutation of *KRAS*

and a nonsynonymous tumor mutation burden of 5 mutations/mb, without any other pathogenic gene alterations. The patient received atezolizumab as a second-line treatment and with a PFS of 21.4 months. The histological type of the resistant tumor was also squamous cell carcinoma. CD8<sup>+</sup> TIL density was initially low, but the Trm-like CD8<sup>+</sup> TIL density (11.5 versus 0–4.1/mm<sup>2</sup>) and PD-1 positivity of CD8<sup>+</sup> TILs (25.0% versus 7.7–18.8%) before ICI treatment (**Fig. 4A**) were higher than those of all nonresponders in cohort-B (**Fig. 2C**). The CD8<sup>+</sup> TIL density declined further after resistance acquisition (from 13.1 to 1.2/mm<sup>2</sup>) (**Fig. 4A**). In addition, the proportion of CD8<sup>+</sup> TILs expressing all co-inhibitory molecules examined (PD-1, TIGIT, LAG-3, TIM-3) increased from 0% to 100% (**Fig. 4A**), suggesting that the small number of tumor-reactive cells had become terminally exhausted, possibly as a result of their repetitive stimulation during long-term tumor control.

Patient 4 was a former smoker with squamous cell carcinoma and a PD-L1 TPS of 80%. This patient received pembrolizumab as a first-line treatment and experienced a PFS of 17.8 months. The histological type of the resistant tumor was also squamous cell carcinoma. CD8<sup>+</sup> TIL density decreased between before and after the acquisition of resistance (from 83.5 to 14.9/mm<sup>2</sup>) (**Fig. 4A** and **D**). The proportion of CD8<sup>+</sup> TILs positive for a Trm-like phenotype increased whereas that of those positive for PD-1 decreased in association with the development of ICI resistance, suggesting that the tumor cells might have at least partially repressed neoantigen presentation and thereby escaped from T cell attack.

Finally, we performed gene expression profiling to evaluate cell signaling signatures in these paired tumor tissue samples from cohort-A (**Fig. 4E**). The pretreatment specimen from patient 1 was excluded from the final analysis because the quality of the extracted RNA did not meet the requirement to proceed (normalization factor was 62.3). Consistent with the mIHC findings, the tumor tissue obtained after resistance acquisition in patient 1 showed enrichment for T cell-related gene expression including the expression of interferon signaling and JAK (Janus kinase)–STAT (signal transducer and activator of transcription) signaling genes. Genes related to antigen presentation and the myeloid compartment were also expressed in the tumor, consistent with the mIHC data showing persistence of tumor-reactive CD8<sup>+</sup> TILs and a marked increase in myeloid cell

density. In addition, signatures for transforming growth factor- $\beta$  signaling and angiogenesis were also enriched, consistent with immunosuppressive and tumorigenic activity of accumulated myeloid cells. The tumor with acquired resistance from patient 3 showed decreased gene expression for signaling pathways related to T cell and myeloid cell activities compared with the pretreatment specimen. Of note, expression of genes for antigen presentation was markedly suppressed, consistent with the mIHC data showing a reduced infiltration of CD8<sup>+</sup> T cells with tumor-antigen reactivity. All signatures for T cells and myeloid cells were upregulated in the tumor sampled after the development of resistance in patient 4, a finding that was not consistent with the mIHC data. This discrepancy might have resulted from contamination by extratumoral tissue in the gene expression analysis, emphasizing the advantage of mIHC with regard to providing spatial information at the single-cell level. In addition, the detection of increased expression of genes related to antigen presentation as opposed to the mIHC results showing decreased infiltration of tumor-reactive CD8<sup>+</sup> T cells was suggestive of a genetic loss of neoantigens in this tumor.

#### **4. Discussion**

Previous studies have suggested important roles for various cell subsets in the TME of solid cancers, but the contributions of these cells to ICI resistance in advanced NSCLC have remained unclear [8, 12]. We have now performed an mIHC-based spatial analysis at the single-cell level to evaluate the detailed immune profiles for tumor tissue of individuals with advanced NSCLC resistant to PD-1/PD-L1 inhibitor treatment. This deep TME profiling included that for paired tumor tissue samples obtained from patients before ICI treatment and after they had acquired resistance to such treatment. Our findings suggest that intratumoral tumor-reactive CD8<sup>+</sup> T cells are a prerequisite for a long-term ICI response in advanced NSCLC, although they are not sufficient to ensure elimination of cancer cells. Changes in TME profiles observed in association with the acquisition of ICI resistance differed among tumors. However, several distinct changes specific for each individual were revealed, suggesting that the mechanisms of primary resistance and those of acquired resistance may differ.

Recent studies have revealed the importance of neoantigen-specific CD8<sup>+</sup> TILs for a tumor

response to ICI treatment. These TILs are characterized by several cell surface molecules including CD39, CD103, and PD-1 [26, 34, 35]. CD8<sup>+</sup> T cells are recruited to tumors by chemokines such as CXCL9, CXCL10, and CXCL11, but these molecules attract T cells nonspecifically, with the result that tumors can also accumulate bystander T cells that are not able to recognize cancer cells [26, 36, 37]. CD39 was shown to be specifically expressed on CD8<sup>+</sup> TILs with T cell receptors that recognize specific neoepitopes [26]. Indeed, a recent study found that the specific expression of CD39 on intratumoral CD8<sup>+</sup> cells was associated with a response to PD-1/PD-L1 blockade in advanced NSCLC [25], with our data now providing further support for this relation. CD103 has also been implicated as an important marker for the identification of neoantigen-specific CD8<sup>+</sup> T cells as clonally expanded Trm cells in solid tumors [38, 39]. The importance of coexpression of CD39 and CD103 on CD8<sup>+</sup> T cells for the identification of neoantigen-specific repertoires in urothelial cancer was suggested by a study based on flow cytometry of intratumoral cells [40], and our data now expand this concept to advanced NSCLC. PD-1 has been recognized as a cell surface marker that is expressed after T cell receptor stimulation by antigen and has been used to select neoantigen-specific CD8<sup>+</sup> T cells from tumors [41, 42]. Indeed, PD-1<sup>+</sup>CD8<sup>+</sup> T cells were found to be associated with a response to PD-1/PD-L1 blockade in melanoma patients [43, 44]. Our study now confirms this relation in NSCLC. Of note, however, we found that the presence of such neoantigen-specific CD8<sup>+</sup> TILs did not guarantee tumor eradication by ICI treatment, as evidenced by the acquired resistance in all four patients of cohort-A. In addition, some patients maintained such neoantigen-specific CD8<sup>+</sup> T cell phenotypes in the tumor nest even after they had acquired resistance to ICI treatment, suggesting that reinvigoration of the tumor-reactive immune cells by some yet to be discovered mechanism might be possible. Indeed, previous studies have suggested that acquired expression of other checkpoint molecules such as TIM-3 or LAG-3 might lead to unresponsiveness of tumor-reactive T cells to PD-1 blockade therapy [45-47]. Our clinical data also suggest that upregulation of these co-inhibitory molecules on CD8<sup>+</sup> TILs might have contributed to the development of acquired resistance to the administered ICIs, and that simultaneous blockade of these molecules in addition to PD-1 might prove effective. Several trials targeting such checkpoint molecules are in progress for

NSCLC [48-50].

Other cell subsets that play an immunosuppressive role have been implicated as potential therapeutic targets by preclinical studies [51, 52]. Tregs are one of the most studied immunosuppressive cell types [53], but they did not appear to be associated with primary or acquired resistance to ICIs in our study. Of interest, CD39 and CD73 expressed specifically on Tregs were suggested to be important for tumor resistance to PD-1/PD-L1 blockade in a mouse study [54]. In addition, PD-1<sup>+</sup> Tregs were suggested to contribute to primary resistance to PD-1 inhibition [55]. These findings indicate the importance of analysis of specific phenotypes of Tregs. Our mIHC analysis allowed the evaluation of Tregs with such specific phenotypes, but neither CD39 nor PD-1 expression on Tregs was associated with ICI resistance in our NSCLC patients. Further studies are needed to clarify the role of these specific cell subsets. The potential roles of immunosuppressive myeloid cells such as TAMs and MDSCs in ICI resistance mechanisms have also been noted [56]. The number of MDSCs was found to increase markedly in association with acquired resistance, as was the proportion of tumor cells expressing CD73, in one patient of our cohort-A. CD73 expression on tumor cells was shown to suppress the antitumor effect of intratumoral T cells via recruitment and activation of MDSCs in a mouse model of pancreatic cancer [32], which might explain our clinical finding. This mouse study also showed that CD73 inhibition could counteract the immunosuppressive effect of MDSCs. Targeting of CD73 is therefore a potential strategy to overcome acquired resistance to ICIs in advanced NSCLC.

Small cell lung cancer transformation of NSCLC has recently been recognized as a potential mechanism of acquired resistance to ICI treatment [57, 58]. Our cohort-A did not show any histological transformation, however, likely reflecting the small number of cases. However, changes in the TME associated with such a histological transformation and the types of immune cells that might contribute to this resistance mechanism warrant further investigation with our approach.

There are several limitations to our study. First, it was retrospective in nature and included only a small number of patients from a single university hospital. Second, genomic analysis was performed for only one tumor specimen obtained from each patient after acquired resistance in

addition to the specimen obtained before treatment. Genetic loss of effective neoantigen presentation by tumor cells is a key event in the development of resistance to ICI treatment [59-62]. However, our study is notable in that it provides a detailed analysis of the TME in advanced NSCLC by spatial profiling of multiple cell subsets at the single-cell level with the use of clinical tumor tissue samples including those obtained after acquired resistance to PD-1/PD-L1 inhibitor treatment. Further studies that apply such mIHC analysis as well as genetic profiling to a larger number of patients are warranted.

## **5. Conclusions**

Our mIHC-based spatial profiling at the single-cell level has suggested that the presence of intratumoral CD8<sup>+</sup> T cells with neoantigen-specific phenotypes is required for a response to PD-1/PD-L1 inhibition in advanced NSCLC. However, such a pretreatment TME profile is not sufficient for tumor eradication by ICI treatment, with the subsequent development of treatment resistance appearing to occur by several different mechanisms in a patient-specific manner. Further studies are needed to develop effective strategies to overcome these individual resistance mechanisms.

## **Funding**

This work was supported by the YOKOYAMA Foundation for Clinical Pharmacology, SGH Foundation, and KANAE Foundation for the Promotion of Medical Science.

## **Acknowledgments**

We thank Mami Kitano, Yume Shinkai, Michiko Kitano, and Haruka Sakamoto of Kindai University, Kyoko Itoh of the Department of Pathology and Applied Neurobiology, Kyoto Prefectural University of Medicine, as well as Hiroshi Ogi and Saya Shibata of SCREEN Holdings Co. Ltd. for their technical support.



## References

- [1] H. Borghaei, L. Paz-Ares, L. Horn, D.R. Spigel, M. Steins, N.E. Ready, L.Q. Chow, E.E. Vokes, E. Felip, E. Holgado, F. Barlesi, M. Kohlhaufl, O. Arrieta, M.A. Burgio, J. Fayette, H. Lena, E. Poddubskaya, D.E. Gerber, S.N. Gettinger, C.M. Rudin, N. Rizvi, L. Crino, G.R. Blumenschein, Jr., S.J. Antonia, C. Dorange, C.T. Harbison, F. Graf Finckenstein, J.R. Brahmer, Nivolumab versus Docetaxel in Advanced Nonsquamous Non-Small-Cell Lung Cancer, *N Engl J Med* 373(17) (2015) 1627-39.
- [2] J. Brahmer, K.L. Reckamp, P. Baas, L. Crino, W.E. Eberhardt, E. Poddubskaya, S. Antonia, A. Pluzanski, E.E. Vokes, E. Holgado, D. Waterhouse, N. Ready, J. Gainor, O. Aren Frontera, L. Havel, M. Steins, M.C. Garassino, J.G. Aerts, M. Domine, L. Paz-Ares, M. Reck, C. Baudelet, C.T. Harbison, B. Lestini, D.R. Spigel, Nivolumab versus Docetaxel in Advanced Squamous-Cell Non-Small-Cell Lung Cancer, *N Engl J Med* 373(2) (2015) 123-35.
- [3] L. Fehrenbacher, A. Spira, M. Ballinger, M. Kowanetz, J. Vansteenkiste, J. Mazieres, K. Park, D. Smith, A. Artal-Cortes, C. Lewanski, F. Braith, D. Waterkamp, P. He, W. Zou, D.S. Chen, J. Yi, A. Sandler, A. Rittmeyer, P.S. Group, Atezolizumab versus docetaxel for patients with previously treated non-small-cell lung cancer (POPLAR): a multicentre, open-label, phase 2 randomised controlled trial, *Lancet* 387(10030) (2016) 1837-46.
- [4] R.S. Herbst, P. Baas, D.W. Kim, E. Felip, J.L. Perez-Gracia, J.Y. Han, J. Molina, J.H. Kim, C.D. Arvis, M.J. Ahn, M. Majem, M.J. Fidler, G. de Castro, Jr., M. Garrido, G.M. Lubiniecki, Y. Shentu, E. Im, M. Dolled-Filhart, E.B. Garon, Pembrolizumab versus docetaxel for previously treated, PD-L1-positive, advanced non-small-cell lung cancer (KEYNOTE-010): a randomised controlled trial, *Lancet* 387(10027) (2016) 1540-1550.
- [5] M. Reck, D. Rodriguez-Abreu, A.G. Robinson, R. Hui, T. Czoszi, A. Fulop, M. Gottfried, N. Peled, A. Tafreshi, S. Cuffe, M. O'Brien, S. Rao, K. Hotta, M.A. Leiby, G.M. Lubiniecki, Y. Shentu, R. Rangwala, J.R. Brahmer, K.-. Investigators,

Pembrolizumab versus Chemotherapy for PD-L1-Positive Non-Small-Cell Lung Cancer, *N Engl J Med* 375(19) (2016) 1823-1833.

[6] A. Rittmeyer, F. Barlesi, D. Waterkamp, K. Park, F. Ciardiello, J. von Pawel, S.M. Gadgeel, T. Hida, D.M. Kowalski, M.C. Dols, D.L. Cortinovis, J. Leach, J. Polikoff, C. Barrios, F. Kabbinavar, O.A. Frontera, F. De Marinis, H. Turna, J.S. Lee, M. Ballinger, M. Kowanetz, P. He, D.S. Chen, A. Sandler, D.R. Gandara, O.A.K.S. Group, Atezolizumab versus docetaxel in patients with previously treated non-small-cell lung cancer (OAK): a phase 3, open-label, multicentre randomised controlled trial, *Lancet* 389(10066) (2017) 255-265.

[7] H. Sung, J. Ferlay, R.L. Siegel, M. Laversanne, I. Soerjomataram, A. Jemal, F. Bray, Global Cancer Statistics 2020: GLOBOCAN Estimates of Incidence and Mortality Worldwide for 36 Cancers in 185 Countries, *CA: A Cancer Journal for Clinicians* 71(3) (2021) 209-249.

[8] A. Passaro, J. Brahmer, S. Antonia, T. Mok, S. Peters, Managing Resistance to Immune Checkpoint Inhibitors in Lung Cancer: Treatment and Novel Strategies, *Journal of Clinical Oncology* 40(6) (2022) 598-610.

[9] F. Li, C. Li, X. Cai, Z. Xie, L. Zhou, B. Cheng, R. Zhong, S. Xiong, J. Li, Z. Chen, Z. Yu, J. He, W. Liang, The association between CD8+ tumor-infiltrating lymphocytes and the clinical outcome of cancer immunotherapy: A systematic review and meta-analysis, *eClinicalMedicine* 41 (2021) 101134.

[10] D.B. Doroshow, S. Bhalla, M.B. Beasley, L.M. Sholl, K.M. Kerr, S. Gnjatic, I.I. Wistuba, D.L. Rimm, M.S. Tsao, F.R. Hirsch, PD-L1 as a biomarker of response to immune-checkpoint inhibitors, *Nature Reviews Clinical Oncology* 18(6) (2021) 345-362.

[11] N.A. Rizvi, M.D. Hellmann, A. Snyder, P. Kvistborg, V. Makarov, J.J. Havel, W. Lee, J. Yuan, P. Wong, T.S. Ho, M.L. Miller, N. Rekhtman, A.L. Moreira, F. Ibrahim, C. Bruggeman, B. Gasmi, R. Zappasodi, Y. Maeda, C. Sander, E.B. Garon, T. Merghoub,

- J.D. Wolchok, T.N. Schumacher, T.A. Chan, Cancer immunology. Mutational landscape determines sensitivity to PD-1 blockade in non-small cell lung cancer, *Science* 348(6230) (2015) 124-8.
- [12] B. Zhou, Y. Gao, P. Zhang, Q. Chu, Acquired Resistance to Immune Checkpoint Blockades: The Underlying Mechanisms and Potential Strategies, *Front Immunol* 12 (2021) 693609.
- [13] D.C. Hinshaw, L.A. Shevde, The Tumor Microenvironment Innately Modulates Cancer Progression, *Cancer Research* 79(18) (2019) 4557-4566.
- [14] W.H. Fridman, L. Zitvogel, C. Sautès-Fridman, G. Kroemer, The immune contexture in cancer prognosis and treatment, *Nature Reviews Clinical Oncology* 14(12) (2017) 717-734.
- [15] F. Klemm, J.A. Joyce, Microenvironmental regulation of therapeutic response in cancer, *Trends Cell Biol* 25(4) (2015) 198-213.
- [16] W.H. Fridman, F. Pagès, C. Sautès-Fridman, J. Galon, The immune contexture in human tumours: impact on clinical outcome, *Nature Reviews Cancer* 12(4) (2012) 298-306.
- [17] T. Tsujikawa, S. Kumar, R.N. Borkar, V. Azimi, G. Thibault, Y.H. Chang, A. Balter, R. Kawashima, G. Choe, D. Sauer, E. El Rassi, D.R. Clayburgh, M.F. Kulesz-Martin, E.R. Lutz, L. Zheng, E.M. Jaffee, P. Leyshock, A.A. Margolin, M. Mori, J.W. Gray, P.W. Flint, L.M. Coussens, Quantitative Multiplex Immunohistochemistry Reveals Myeloid-Inflamed Tumor-Immune Complexity Associated with Poor Prognosis, *Cell Rep* 19(1) (2017) 203-217.
- [18] T. Tsujikawa, T. Crocenzi, J.N. Durham, E.A. Sugar, A.A. Wu, B. Onners, J.M. Nauroth, R.A. Anders, E.J. Fertig, D.A. Laheru, K. Reiss, R.H. Vonderheide, A.H. Ko, M.A. Tempero, G.A. Fisher, M. Considine, L. Danilova, D.G. Brockstedt, L.M. Coussens, E.M. Jaffee, D.T. Le, Evaluation of Cyclophosphamide/GVAX Pancreas Followed by Listeria-Mesothelin (CRS-207) with or without Nivolumab in Patients

with Pancreatic Cancer, *Clinical Cancer Research* 26(14) (2020) 3578-3588.

[19] V. Gopalakrishnan, C.N. Spencer, L. Nezi, A. Reuben, M.C. Andrews, T.V. Karpinets, P.A. Prieto, D. Vicente, K. Hoffman, S.C. Wei, A.P. Cogdill, L. Zhao, C.W. Hudgens, D.S. Hutchinson, T. Manzo, M. Petaccia de Macedo, T. Cotechini, T. Kumar, W.S. Chen, S.M. Reddy, R. Szczepaniak Sloane, J. Galloway-Pena, H. Jiang, P.L. Chen, E.J. Shpall, K. Rezvani, A.M. Alousi, R.F. Chemaly, S. Shelburne, L.M. Vence, P.C. Okhuysen, V.B. Jensen, A.G. Swennes, F. McAllister, E. Marcelo Riquelme Sanchez, Y. Zhang, E. Le Chatelier, L. Zitvogel, N. Pons, J.L. Austin-Breneman, L.E. Haydu, E.M. Burton, J.M. Gardner, E. Sirmans, J. Hu, A.J. Lazar, T. Tsujikawa, A. Diab, H. Tawbi, I.C. Glitza, W.J. Hwu, S.P. Patel, S.E. Woodman, R.N. Amaria, M.A. Davies, J.E. Gershenwald, P. Hwu, J.E. Lee, J. Zhang, L.M. Coussens, Z.A. Cooper, P.A. Futreal, C.R. Daniel, N.J. Ajami, J.F. Petrosino, M.T. Tetzlaff, P. Sharma, J.P. Allison, R.R. Jenq, J.A. Wargo, Gut microbiome modulates response to anti-PD-1 immunotherapy in melanoma patients, *Science* 359(6371) (2018) 97-103.

[20] K. Yoshimura, T. Tsujikawa, J. Mitsuda, H. Ogi, S. Saburi, G. Ohmura, A. Arai, S. Shibata, G. Thibault, Y.H. Chang, D.R. Clayburgh, S. Yasukawa, A. Miyagawa-Hayashino, E. Konishi, K. Itoh, L.M. Coussens, S. Hirano, Spatial Profiles of Intratumoral PD-1(+) Helper T Cells Predict Prognosis in Head and Neck Squamous Cell Carcinoma, *Front Immunol* 12 (2021) 769534.

[21] K. Haratani, H. Hayashi, T. Takahama, Y. Nakamura, S. Tomida, T. Yoshida, Y. Chiba, T. Sawada, K. Sakai, Y. Fujita, Y. Togashi, J. Tanizaki, H. Kawakami, A. Ito, K. Nishio, K. Nakagawa, Clinical and immune profiling for cancer of unknown primary site, *J Immunother Cancer* 7(1) (2019) 251.

[22] T. Gruosso, M. Gigoux, V.S.K. Manem, N. Bertos, D. Zuo, I. Perlitch, S.M.I. Saleh, H. Zhao, M. Souleimanova, R.M. Johnson, A. Monette, V.M. Ramos, M.T. Hallett, J. Stagg, R. Lapointe, A. Omeroglu, S. Meterissian, L. Buisseret, G. Van Den Eyden, R. Salgado, M.-C. Guiot, B. Haibe-Kains, M. Park, Spatially distinct tumor immune

microenvironments stratify triple-negative breast cancers, *Journal of Clinical Investigation* 129(4) (2019) 1785-1800.

[23] N.C. Blessin, W. Li, T. Mandelkow, H.L. Jansen, C. Yang, J.B. Raedler, R. Simon, F. Büscheck, D. Dum, A.M. Luebke, A. Hinsch, K. Möller, A. Menz, C. Bernreuther, P. Lebok, T. Clauditz, G. Sauter, A. Marx, R. Uhlig, W. Wilczak, S. Minner, T. Krech, C. Fraune, D. Höflmayer, E. Burandt, S. Steurer, Prognostic role of proliferating CD8+ cytotoxic T cells in human cancers, *Cellular Oncology* 44(4) (2021) 793-803.

[24] A.M. Mulligan, D. Pinnaduwa, S. Tchatchou, S.B. Bull, I.L. Andrulis, Validation of Intratumoral T-bet+ Lymphoid Cells as Predictors of Disease-Free Survival in Breast Cancer, *Cancer Immunology Research* 4(1) (2016) 41-48.

[25] J. Yeong, L. Suteja, Y. Simoni, K.W. Lau, A.C. Tan, H.H. Li, S. Lim, J.H. Loh, F.Y.T. Wee, S.N. Nerurkar, A. Takano, E.H. Tan, T.K.H. Lim, E.W. Newell, D.S.W. Tan, Intratumoral CD39(+)/CD8(+) T Cells Predict Response to Programmed Cell Death Protein-1 or Programmed Death Ligand-1 Blockade in Patients With NSCLC, *J Thorac Oncol* 16(8) (2021) 1349-1358.

[26] Y. Simoni, E. Becht, M. Fehlings, C.Y. Loh, S.L. Koo, K.W.W. Teng, J.P.S. Yeong, R. Nahar, T. Zhang, H. Kared, K. Duan, N. Ang, M. Poidinger, Y.Y. Lee, A. Larbi, A.J. Khng, E. Tan, C. Fu, R. Mathew, M. Teo, W.T. Lim, C.K. Toh, B.H. Ong, T. Koh, A.M. Hillmer, A. Takano, T.K.H. Lim, E.H. Tan, W. Zhai, D.S.W. Tan, I.B. Tan, E.W. Newell, Bystander CD8(+) T cells are abundant and phenotypically distinct in human tumour infiltrates, *Nature* 557(7706) (2018) 575-579.

[27] M. Binnewies, E.W. Roberts, K. Kersten, V. Chan, D.F. Fearon, M. Merad, L.M. Coussens, D.I. Gabrilovich, S. Ostrand-Rosenberg, C.C. Hedrick, R.H. Vonderheide, M.J. Pittet, R.K. Jain, W. Zou, T.K. Howcroft, E.C. Woodhouse, R.A. Weinberg, M.F. Krummel, Understanding the tumor immune microenvironment (TIME) for effective therapy, *Nat Med* 24(5) (2018) 541-550.

[28] P. Sharma, S. Hu-Lieskovan, J.A. Wargo, A. Ribas, Primary, Adaptive, and

- Acquired Resistance to Cancer Immunotherapy, *Cell* 168(4) (2017) 707-723.
- [29] M. Pitt, Jonathan, M. Vétizou, R. Daillère, P. Roberti, María, T. Yamazaki, B. Routy, P. Lepage, G. Boneca, Ivo, M. Chamaillard, G. Kroemer, L. Zitvogel, Resistance Mechanisms to Immune-Checkpoint Blockade in Cancer: Tumor-Intrinsic and - Extrinsic Factors, *Immunity* 44(6) (2016) 1255-1269.
- [30] B. Allard, S. Pommey, M.J. Smyth, J. Stagg, Targeting CD73 Enhances the Antitumor Activity of Anti-PD-1 and Anti-CTLA-4 mAbs, *Clinical Cancer Research* 19(20) (2013) 5626-5635.
- [31] D. Cai, J. Li, D. Liu, S. Hong, Q. Qiao, Q. Sun, P. Li, N. Lyu, T. Sun, S. Xie, L. Guo, L. Ni, L. Jin, C. Dong, Tumor-expressed B7-H3 mediates the inhibition of antitumor T-cell functions in ovarian cancer insensitive to PD-1 blockade therapy, *Cellular & Molecular Immunology* 17(3) (2020) 227-236.
- [32] R.J. King, S.K. Shukla, C. He, E. Vernucci, R. Thakur, K.S. Attri, A. Dasgupta, N.V. Chaika, S.E. Mulder, J. Abrego, D. Murthy, V. Gunda, C.G. Pacheco, P.M. Grandgenett, A.J. Lazenby, M.A. Hollingsworth, F. Yu, K. Mehla, P.K. Singh, CD73 induces GM-CSF/MDSC-mediated suppression of T cells to accelerate pancreatic cancer pathogenesis, *Oncogene* 41(7) (2022) 971-982.
- [33] I. Montalbán Del Barrio, C. Penski, L. Schlahsa, R.G. Stein, J. Diessner, A. Wöckel, J. Dietl, M.B. Lutz, M. Mittelbronn, J. Wischhusen, S.F.M. Häusler, Adenosine-generating ovarian cancer cells attract myeloid cells which differentiate into adenosine-generating tumor associated macrophages – a self-amplifying, CD39- and CD73-dependent mechanism for tumor immune escape, *Journal for ImmunoTherapy of Cancer* 4(1) (2016).
- [34] S.N. Mueller, L.K. Mackay, Tissue-resident memory T cells: local specialists in immune defence, *Nature Reviews Immunology* 16(2) (2016) 79-89.
- [35] A. Gros, P.F. Robbins, X. Yao, Y.F. Li, S. Turcotte, E. Tran, J.R. Wunderlich, A. Mixon, S. Farid, M.E. Dudley, K.-I. Hanada, J.R. Almeida, S. Darko, D.C. Douek, J.C.

- Yang, S.A. Rosenberg, PD-1 identifies the patient-specific CD8+ tumor-reactive repertoire infiltrating human tumors, *Journal of Clinical Investigation* 124(5) (2014) 2246-2259.
- [36] R. Tokunaga, W. Zhang, M. Naseem, A. Puccini, M.D. Berger, S. Soni, M. Mcskane, H. Baba, H.-J. Lenz, CXCL9, CXCL10, CXCL11/CXCR3 axis for immune activation – A target for novel cancer therapy, *Cancer Treatment Reviews* 63 (2018) 40-47.
- [37] K. Franciszkiewicz, A. Boissonnas, M. Boutet, C. Combadière, F. Mami-Chouaib, Role of Chemokines and Chemokine Receptors in Shaping the Effector Phase of the Antitumor Immune Response, *Cancer Research* 72(24) (2012) 6325-6332.
- [38] S. Cognac, I. Damei, G. Gros, A. Caidi, S. Terry, S. Chouaib, M. Deloger, F. Mami-Chouaib, Cancer stem-like cells evade CD8(+)CD103(+) tumor-resident memory T (TRM) lymphocytes by initiating an epithelial-to-mesenchymal transition program in a human lung tumor model, *J Immunother Cancer* 10(4) (2022) e004527.
- [39] F. Djenidi, J. Adam, A. Goubar, A. Durgeau, G. Meurice, V. De Montpréville, P. Validire, B. Besse, F. Mami-Chouaib, CD8+CD103+Tumor-Infiltrating Lymphocytes Are Tumor-Specific Tissue-Resident Memory T Cells and a Prognostic Factor for Survival in Lung Cancer Patients, *The Journal of Immunology* 194(7) (2015) 3475-3486.
- [40] T. Duhén, R. Duhén, R. Montler, J. Moses, T. Moudgil, N.F. De Miranda, C.P. Goodall, T.C. Blair, B.A. Fox, J.E. Mcdermott, S.-C. Chang, G. Grunkemeier, R. Leidner, R.B. Bell, A.D. Weinberg, Co-expression of CD39 and CD103 identifies tumor-reactive CD8 T cells in human solid tumors, *Nature Communications* 9(1) (2018).
- [41] A. Gros, E. Tran, M.R. Parkhurst, S. Ilyas, A. Pasetto, E.M. Groh, P.F. Robbins, R. Yossef, A. Garcia-Garijo, C.A. Fajardo, T.D. Prickett, L. Jia, J.J. Gartner, S. Ray, L. Ngo, J.R. Wunderlich, J.C. Yang, S.A. Rosenberg, Recognition of human gastrointestinal cancer neoantigens by circulating PD-1+ lymphocytes, *Journal of Clinical Investigation* 129(11) (2019) 4992-5004.

- [42] E. Tran, M. Ahmadzadeh, Y.C. Lu, A. Gros, S. Turcotte, P.F. Robbins, J.J. Gartner, Z. Zheng, Y.F. Li, S. Ray, J.R. Wunderlich, R.P. Somerville, S.A. Rosenberg, Immunogenicity of somatic mutations in human gastrointestinal cancers, *Science* 350(6266) (2015) 1387-90.
- [43] A.I. Daud, K. Loo, M.L. Pauli, R. Sanchez-Rodriguez, P.M. Sandoval, K. Taravati, K. Tsai, A. Nosrati, L. Nardo, M.D. Alvarado, A.P. Algazi, M.H. Pampaloni, I.V. Lobach, J. Hwang, R.H. Pierce, I.K. Gratz, M.F. Krummel, M.D. Rosenblum, Tumor immune profiling predicts response to anti-PD-1 therapy in human melanoma, *J Clin Invest* 126(9) (2016) 3447-52.
- [44] P.C. Tumeh, C.L. Harview, J.H. Yearley, I.P. Shintaku, E.J.M. Taylor, L. Robert, B. Chmielowski, M. Spasic, G. Henry, V. Ciobanu, A.N. West, M. Carmona, C. Kivork, E. Seja, G. Cherry, A.J. Gutierrez, T.R. Grogan, C. Mateus, G. Tomasic, J.A. Glaspy, R.O. Emerson, H. Robins, R.H. Pierce, D.A. Elashoff, C. Robert, A. Ribas, PD-1 blockade induces responses by inhibiting adaptive immune resistance, *Nature* 515(7528) (2014) 568-571.
- [45] S. Koyama, E.A. Akbay, Y.Y. Li, G.S. Herter-Sprie, K.A. Buczkowski, W.G. Richards, L. Gandhi, A.J. Redig, S.J. Rodig, H. Asahina, R.E. Jones, M.M. Kulkarni, M. Kuraguchi, S. Palakurthi, P.E. Fecci, B.E. Johnson, P.A. Janne, J.A. Engelman, S.P. Gangadharan, D.B. Costa, G.J. Freeman, R. Bueno, F.S. Hodi, G. Dranoff, K.K. Wong, P.S. Hammerman, Adaptive resistance to therapeutic PD-1 blockade is associated with upregulation of alternative immune checkpoints, *Nat Commun* 7 (2016) 10501.
- [46] A. Oweida, M.K. Hararah, A. Phan, D. Binder, S. Bhatia, S. Lennon, S. Bukkapatnam, B. Van Court, N. Uyanga, L. Darragh, H.M. Kim, D. Raben, A.C. Tan, L. Heasley, E. Clambey, R. Nemenoff, S.D. Karam, Resistance to Radiotherapy and PD-L1 Blockade Is Mediated by TIM-3 Upregulation and Regulatory T-Cell Infiltration, *Clin Cancer Res* 24(21) (2018) 5368-5380.
- [47] D.B. Johnson, M.J. Nixon, Y. Wang, D.Y. Wang, E. Castellanos, M.V. Estrada, P.I.



Ericsson-Gonzalez, C.H. Cote, R. Salgado, V. Sanchez, P.T. Dean, S.R. Opalenik, D.M. Schreeder, D.L. Rimm, J.Y. Kim, J. Bordeaux, S. Loi, L. Horn, M.E. Sanders, P.B. Ferrell, Y. Xu, J.A. Sosman, R.S. Davis, J.M. Balko, Tumor-specific MHC-II expression drives a unique pattern of resistance to immunotherapy via LAG-3/FCRL6 engagement, *JCI Insight* 3(24) (2018) e120360.

[48] P. Schöffski, D.S.W. Tan, M. Martín, M. Ochoa-De-Olza, J. Sarantopoulos, R.D. Carvajal, C. Kyi, T. Esaki, A. Prawira, W. Akerley, F. De Braud, R. Hui, T. Zhang, R.A. Soo, M. Maur, A. Weickhardt, J. Krauss, B. Deschler-Baier, A. Lau, T.S. Samant, T. Longmire, N.R. Chowdhury, C.A. Sabatos-Peyton, N. Patel, R. Ramesh, T. Hu, A. Carion, D. Gusenleitner, P. Yerramilli-Rao, V. Askoxylakis, E.L. Kwak, D.S. Hong, Phase I/II study of the LAG-3 inhibitor ieramilimab (LAG525) ± anti-PD-1 spartalizumab (PDR001) in patients with advanced malignancies, *Journal for ImmunoTherapy of Cancer* 10(2) (2022) e003776.

[49] J. Niu, C. Maurice-Dror, D.H. Lee, D.-W. Kim, A. Nagrial, M. Voskoboynik, H.C. Chung, K. Mileham, U. Vaishampayan, D. Rasco, T. Golan, T.M. Bauer, A. Jimeno, V. Chung, E. Chartash, M. Lala, Q. Chen, J.A. Healy, M.-J. Ahn, First-in-human phase 1 study of the anti-TIGIT antibody vibostolimab as monotherapy or with pembrolizumab for advanced solid tumors, including non-small-cell lung cancer, *Annals of Oncology* 33(2) (2022) 169-180.

[50] G. Curigliano, H. Gelderblom, N. Mach, T. Doi, D. Tai, P.M. Forde, J. Sarantopoulos, P.L. Bedard, C.-C. Lin, F.S. Hodi, S. Wilgenhof, A. Santoro, C.A. Sabatos-Peyton, T.A. Longmire, A. Xyrafas, H. Sun, S. Gutzwiller, L. Manenti, A. Naing, Phase I/Ib Clinical Trial of Sabatolimab, an Anti-TIM-3 Antibody, Alone and in Combination with Spartalizumab, an Anti-PD-1 Antibody, in Advanced Solid Tumors, *Clinical Cancer Research* 27(13) (2021) 3620-3629.

[51] X. Mao, J. Xu, W. Wang, C. Liang, J. Hua, J. Liu, B. Zhang, Q. Meng, X. Yu, S. Shi, Crosstalk between cancer-associated fibroblasts and immune cells in the tumor

microenvironment: new findings and future perspectives, *Molecular Cancer* 20(1) (2021).

[52] V. Kumar, S. Patel, E. Tcyganov, D.I. Gabrilovich, The Nature of Myeloid-Derived Suppressor Cells in the Tumor Microenvironment, *Trends in Immunology* 37(3) (2016) 208-220.

[53] A. Tanaka, S. Sakaguchi, Regulatory T cells in cancer immunotherapy, *Cell Research* 27(1) (2017) 109-118.

[54] T. Maj, W. Wang, J. Crespo, H. Zhang, W. Wang, S. Wei, L. Zhao, L. Vatan, I. Shao, W. Szeliga, C. Lyssiotis, J.R. Liu, I. Kryczek, W. Zou, Oxidative stress controls regulatory T cell apoptosis and suppressor activity and PD-L1-blockade resistance in tumor, *Nature Immunology* 18(12) (2017) 1332-1341.

[55] S. Kumagai, Y. Togashi, T. Kamada, E. Sugiyama, H. Nishinakamura, Y. Takeuchi, K. Vitaly, K. Itahashi, Y. Maeda, S. Matsui, T. Shibahara, Y. Yamashita, T. Irie, A. Tsuge, S. Fukuoka, A. Kawazoe, H. Udagawa, K. Kirita, K. Aokage, G. Ishii, T. Kuwata, K. Nakama, M. Kawazu, T. Ueno, N. Yamazaki, K. Goto, M. Tsuboi, H. Mano, T. Doi, K. Shitara, H. Nishikawa, The PD-1 expression balance between effector and regulatory T cells predicts the clinical efficacy of PD-1 blockade therapies, *Nat Immunol* 21(11) (2020) 1346-1358.

[56] E. Lebegge, S.M. Arnouk, P.M.R. Bardet, M. Kiss, G. Raes, J.A. Van Ginderachter, Innate Immune Defense Mechanisms by Myeloid Cells That Hamper Cancer Immunotherapy, *Front Immunol* 11 (2020) 1395.

[57] W.T. Iams, K.E. Beckermann, K. Almodovar, J. Hernandez, C. Vnencak-Jones, L.P. Lim, C.K. Raymond, L. Horn, C.M. Lovly, Small Cell Lung Cancer Transformation as a Mechanism of Resistance to PD-1 Therapy in KRAS-Mutant Lung Adenocarcinoma: A Report of Two Cases, *J Thorac Oncol* 14(3) (2019) e45-e48.

[58] K. Sehgal, A. Varkaris, H. Viray, P.A. VanderLaan, D. Rangachari, D.B. Costa, Small cell transformation of non-small cell lung cancer on immune checkpoint

inhibitors: uncommon or under-recognized?, *J Immunother Cancer* 8(1) (2020) e000697.

[59] V. Anagnostou, P.M. Forde, J.R. White, N. Niknafs, C. Hruban, J. Naidoo, K. Marrone, I.K.A. Sivakumar, D.C. Bruhm, S. Rosner, J. Phallen, A. Leal, V. Adleff, K.N. Smith, T.R. Cottrell, L. Rhymee, D.N. Palsgrove, C.L. Hann, B. Levy, J. Feliciano, C. Georgiades, F. Verde, P. Illei, Q.K. Li, E. Gabrielson, M.V. Brock, J.M. Isbell, J.L. Sauter, J. Taube, R.B. Scharpf, R. Karchin, D.M. Pardoll, J.E. Chaft, M.D. Hellmann, J.R. Brahmer, V.E. Velculescu, Dynamics of Tumor and Immune Responses during Immune Checkpoint Blockade in Non–Small Cell Lung Cancer, *Cancer Research* 79(6) (2019) 1214-1225.

[60] M. Sade-Feldman, Y.J. Jiao, J.H. Chen, M.S. Rooney, M. Barzily-Rokni, J.-P. Eliane, S.L. Bjorgaard, M.R. Hammond, H. Vitzthum, S.M. Blackmon, D.T. Frederick, M. Hazar-Rethinam, B.A. Nadres, E.E. Van Seventer, S.A. Shukla, K. Yizhak, J.P. Ray, D. Rosebrock, D. Livitz, V. Adalsteinsson, G. Getz, L.M. Duncan, B. Li, R.B. Corcoran, D.P. Lawrence, A. Stemmer-Rachamimov, G.M. Boland, D.A. Landau, K.T. Flaherty, R.J. Sullivan, N. Hacohen, Resistance to checkpoint blockade therapy through inactivation of antigen presentation, *Nature Communications* 8(1) (2017).

[61] S. Gettinger, J. Choi, K. Hastings, A. Truini, I. Datar, R. Sowell, A. Wurtz, W. Dong, G. Cai, M.A. Melnick, V.Y. Du, J. Schlessinger, S.B. Goldberg, A. Chiang, M.F. Sanmamed, I. Melero, J. Agorreta, L.M. Montuenga, R. Lifton, S. Ferrone, P. Kavathas, D.L. Rimm, S.M. Kaech, K. Schalper, R.S. Herbst, K. Politi, Impaired HLA Class I Antigen Processing and Presentation as a Mechanism of Acquired Resistance to Immune Checkpoint Inhibitors in Lung Cancer, *Cancer Discovery* 7(12) (2017) 1420-1435.

[62] J.M. Zaretsky, A. Garcia-Diaz, D.S. Shin, H. Escuin-Ordinas, W. Hugo, S. Hu-Lieskovan, D.Y. Torrejon, G. Abril-Rodriguez, S. Sandoval, L. Barthly, J. Saco, B. Homet Moreno, R. Mezzadra, B. Chmielowski, K. Ruchalski, I.P. Shintaku, P.J. Sanchez, C. Puig-Saus, G. Cherry, E. Seja, X. Kong, J. Pang, B. Berent-Maoz, B.

Comin-Anduix, T.G. Graeber, P.C. Tumei, T.N.M. Schumacher, R.S. Lo, A. Ribas,  
Mutations Associated with Acquired Resistance to PD-1 Blockade in Melanoma, New  
England Journal of Medicine 375(9) (2016) 819-829.

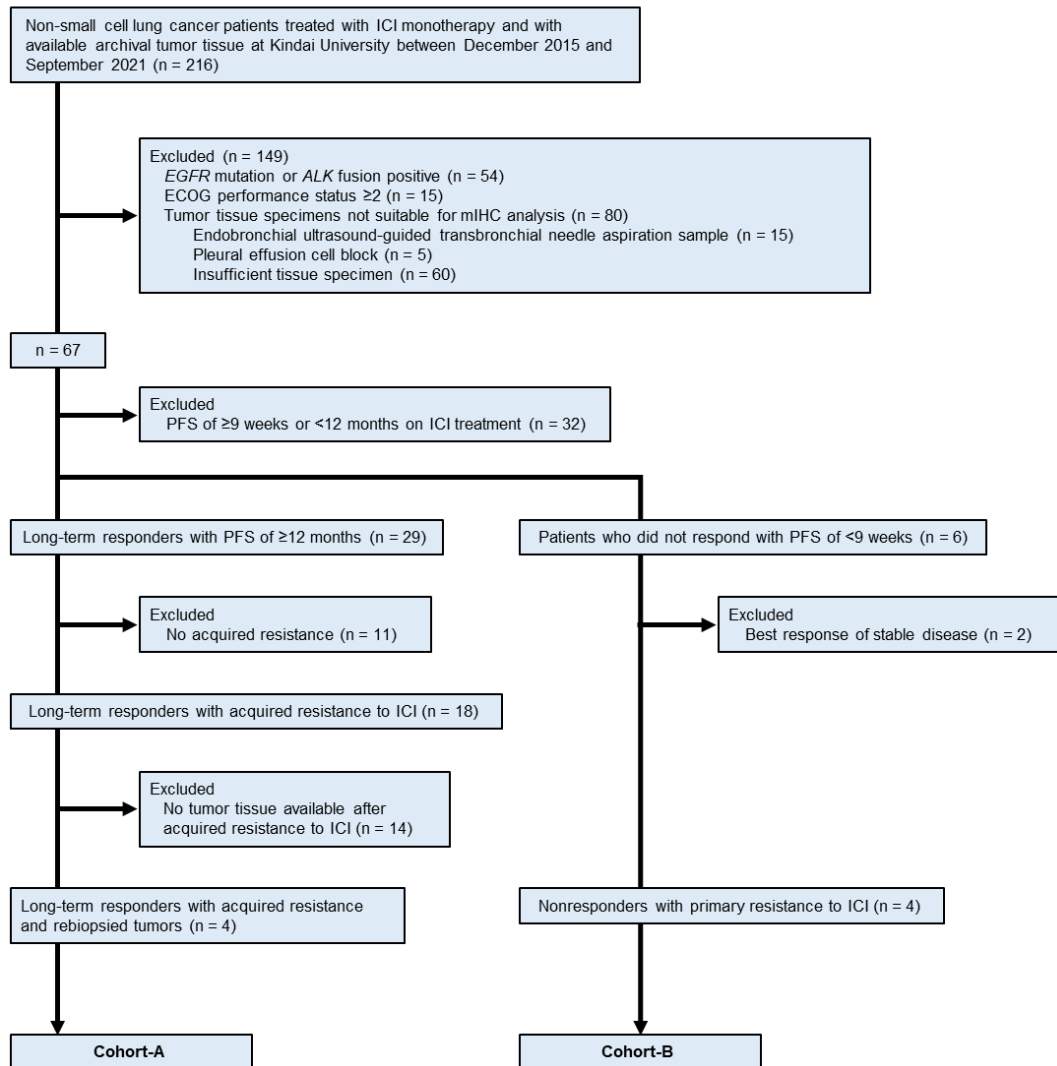
**Table 1. Patient characteristics**

Characteristic	All patients ( <i>n</i> = 8)	Cohort-A ( <i>n</i> = 4)	Cohort-B ( <i>n</i> = 4)
Median age (range), years	71 (53–76)	70 (65–76)	71 (53–75)
Sex			
Male	7 (87.5)	3 (75)	4 (100)
Female	1 (12.5)	1 (25)	0 (0)
ECOG performance status			
0	2 (25)	1 (25)	1 (25)
1	6 (75)	3 (75)	3 (75)
Smoking status <sup>a</sup>			
Current or former	7 (87.5)	3 (75)	4 (100)
Never	1 (12.5)	1 (25)	0 (0)
Histology			
Adenocarcinoma	2 (25)	2 (50)	0 (0)
Squamous	6 (75)	2 (50)	4 (100)
PD-L1 TPS			
≥50%	2 (25)	1 (25)	1 (25)
1–49%	2 (25)	1 (25)	1 (25)
<1%	2 (25)	1 (25)	1 (25)
Unknown	2 (25)	1 (25)	1 (25)
PD-1/PD-L1 antibody			
Nivolumab	5 (62.5)	3 (75)	2 (50)
Pembrolizumab	2 (25)	1 (25)	1 (25)
Atezolizumab	1 (12.5)	0 (0)	1 (25)
PD-1/PD-L1 antibody treatment line			
1	1 (12.5)	1 (25)	0 (0)
2	6 (75)	2 (50)	4 (100)
3	1 (12.5)	1 (25)	0 (0)
Median PFS (range), days	298.5 (35–763)	618.5 (535–763)	42 (35–62)

All data with the exception of age and PFS are *n* (%). Abbreviations: ECOG, Eastern Cooperative Oncology Group; PD-L1 TPS, programmed cell death–ligand 1 tumor proportion score; PD-1, programmed cell death–1; PFS, progression-free survival.

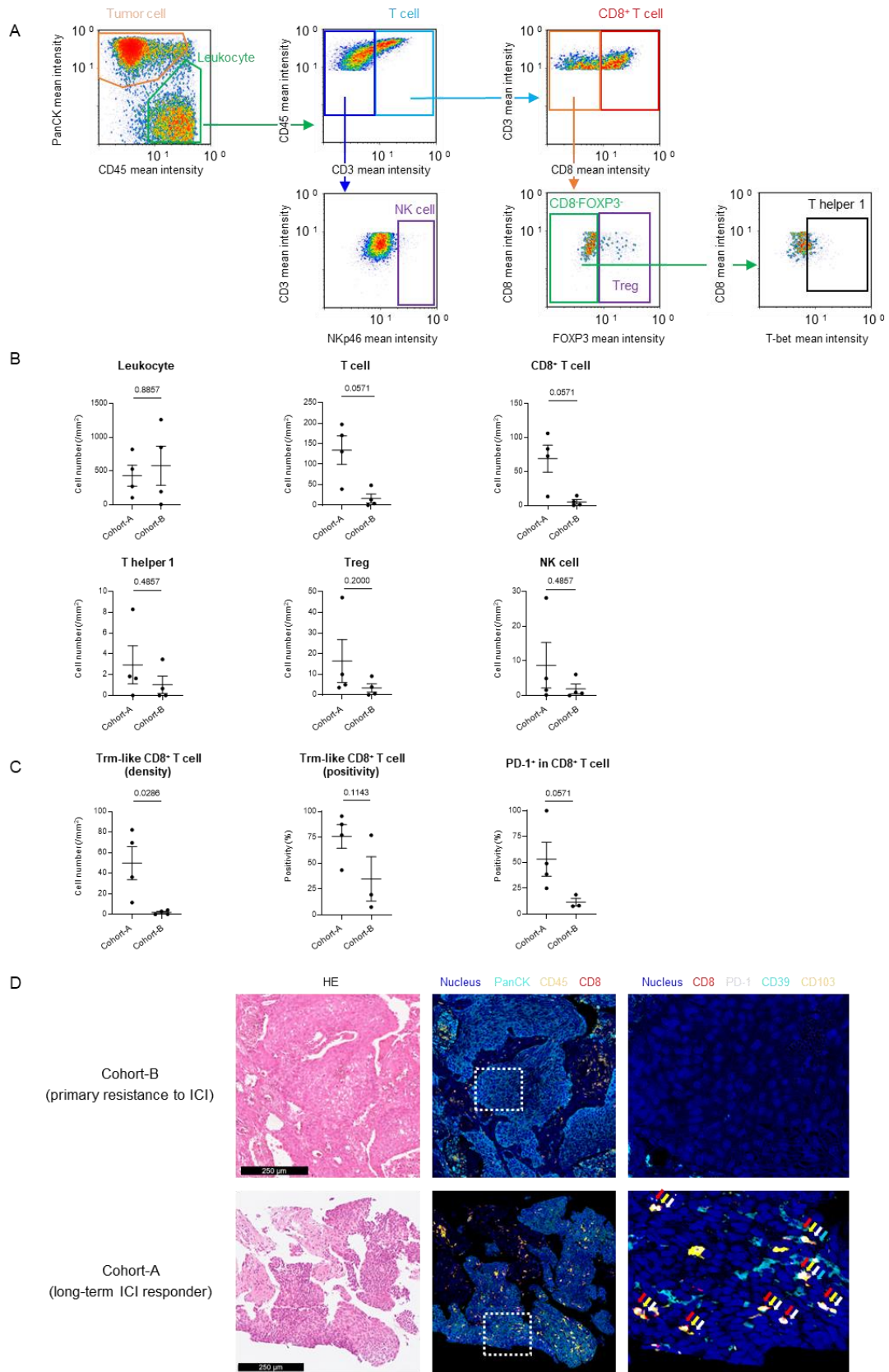
<sup>a</sup>Current smokers were defined as individuals who had smoked a cigarette within the previous year, former smokers as those who had smoked ≥100 cigarettes but had quit >1 year before initiation of PD-1/PD-L1 antibody treatment, and never-smokers as those who had smoked <100 cigarettes.

Fig. 1



**Fig. 1. Flow diagram for patient selection.** ICI, immune checkpoint inhibitor; *EGFR*, epidermal growth factor receptor gene; *ALK*, anaplastic lymphoma kinase gene; ECOG, Eastern Cooperative Oncology Group; mIHC, multiplex immunohistochemistry; PFS, progression-free survival.

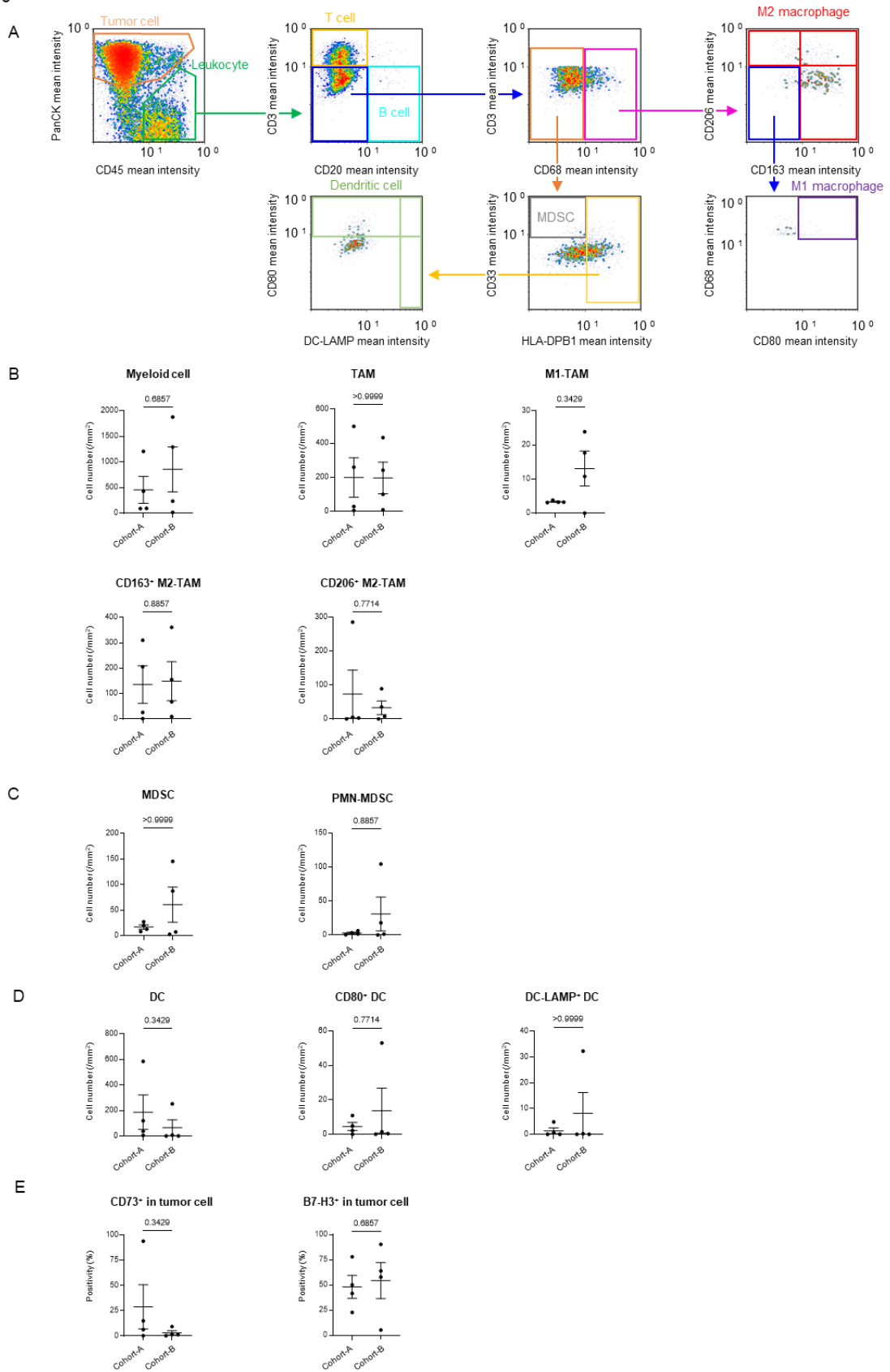
Fig. 2



**Fig. 2. Multiplex immunohistochemistry (mIHC)–based quantitative single-cell analysis of intratumoral lymphocytes.** (A) Gating strategy for evaluation of lymphocytes including natural killer (NK) cells and regulatory T cells (Tregs) in the tumor nest. (B) Densities of intratumoral lymphocytes in cohort-A and cohort-B. (C) Density of Trm-like (CD39<sup>+</sup>CD103<sup>+</sup>) CD8<sup>+</sup> T cells and the proportion of Trm-like or PD-1<sup>+</sup> cells among CD8<sup>+</sup> T cells. Data in (B) and (C) indicate the mean  $\pm$  standard error of the mean (SEM). The *P* values for comparisons between the two cohorts were determined with the Mann-Whitney U test. (D) Representative mIHC images of tumor tissue specimens from patients in cohort-A and cohort-B. Trm-like CD8<sup>+</sup> T cells were more abundant in the tumor from cohort-A than in that from cohort-B. Hematoxylin-eosin (HE) staining is shown in the left column, and corresponding multicolor images showing the nucleus (blue), PanCK (cyan), CD45 (yellow), and CD8 (red) are shown in the middle column. The boxed regions of the middle panels are shown at higher magnification in the right column, with the nucleus (blue), CD8 (red), PD-1 (gray), CD39 (cyan), and CD103 (yellow) being indicated. Arrows represent overlapping color markers. Scale bars, 250  $\mu$ m. PanCK, pan-cytokeratin; FOXP3, forkhead box P3; T-bet, T-box expressed in T cells; Trm, tissue-resident memory; PD-1, programmed cell death–1; ICI, immune checkpoint inhibitor.

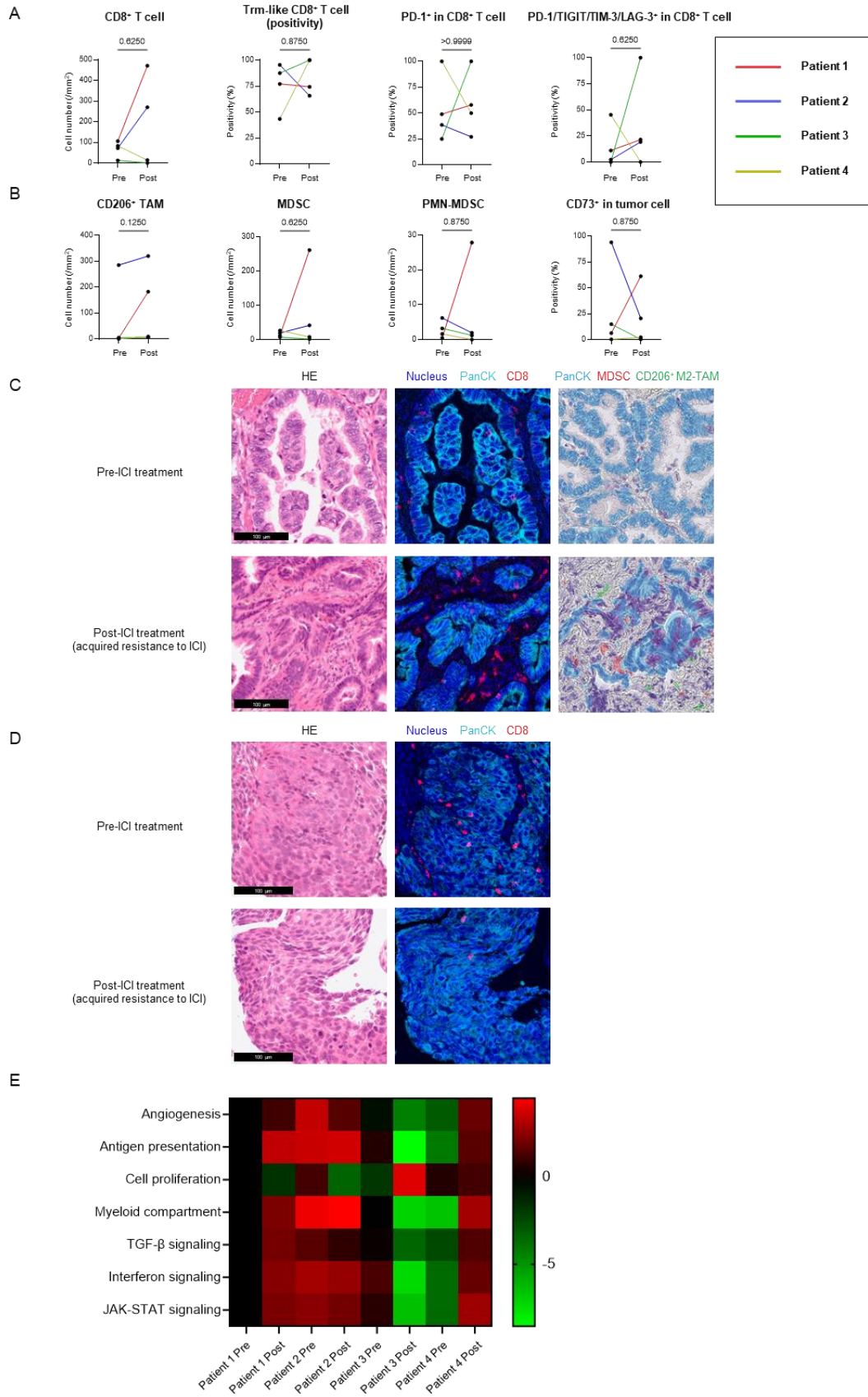


Fig. 3



**Fig. 3. Multiplex immunohistochemistry–based quantitative single-cell analysis of intratumoral myeloid cells.** (A) Gating strategy for evaluation of myeloid cells in the tumor nest. (B–D) Densities of tumor-associated macrophages (TAMs), myeloid-derived suppressor cells (MDSCs), and dendritic cells (DCs), respectively, in cohort-A and cohort-B. (E) CD73 and B7-H3 expression positivity for tumor cells in cohort-A and cohort-B. Data in (B) to (E) indicate the mean  $\pm$  standard error of the mean (SEM), and the *P* values for comparisons between the two cohorts were determined with the Mann-Whitney U test. PanCK, pan-cytokeratin; LAMP, lysosome-associated membrane protein; HLA-DPB1, human leukocyte antigen–DPB1; PMN, polymorphonuclear.

Fig. 4



**Fig. 4. Multiplex immunohistochemistry (mIHC)–based quantification of various cell lineages before and after acquired resistance to immune checkpoint inhibitor (ICI) treatment.** (A) Changes in intratumoral CD8<sup>+</sup> T cell phenotypes between before treatment (pre) and after the development of ICI resistance (post) in individual patients of cohort-A. (B) Changes in tumor-associated macrophage (TAM) density, myeloid-derived suppressor cell (MDSC) density, and CD73 expression in tumor cells for patients as in (A). The *P* values in (A) and (B) were determined with the Wilcoxon signed rank test for pairwise comparisons. (C) Representative mIHC images for patient 1. Hematoxylin-eosin (HE) staining before ICI treatment (upper) and after acquired resistance to such treatment (lower) is shown in the left column, and corresponding multicolor images with the nucleus (blue), pan-cytokeratin (PanCK, cyan), and CD8 (red) are shown in the middle column. Multicolor images generated by layering of colors for MDSCs (red) and CD206<sup>+</sup> TAMs (green) on hematoxylin images are shown in the right column. Note that CD8<sup>+</sup> cells had infiltrated the tumor nest both before and after ICI treatment, whereas MDSCs and TAMs had infiltrated only after treatment. (D) Representative mIHC images for patient 4. HE staining before (upper) and after (lower) acquired resistance to ICI treatment is shown in the left column, and corresponding multicolor images with the nucleus (blue), PanCK (cyan), and CD8 (red) are shown in the right column. The number of CD8<sup>+</sup> cells was decreased after ICI treatment. Scale bars in (C) and (D), 100 μm. (E) Heat map showing gene signature scores of seven pathways for tumor samples obtained before and after acquired resistance to ICI treatment in the individual patients of cohort-A. Each colored square represents the Z score, with the highest expression shown in red, median in black, and lowest in green. The sample obtained from patient 1 before treatment was not suitable for analysis. Trm, tissue-resident memory; PD-1, programmed cell death-1; TIGIT, T cell immunoreceptor with immunoglobulin and ITIM domains; TIM-3, T cell immunoglobulin and mucin domain containing-3; LAG-3, lymphocyte activation gene-3; PMN, polymorphonuclear; TGF-β, transforming growth factor-β; JAK-STAT, Janus kinase–signal transducer and activator of transcription.

## Supplementary Table S1. Details of the multiplex immunohistochemistry panels adopted in this study.

Panel 1

	Round 1	Round 2	Round 3	Round 4	Round 5	Round 6	Round 7	Round 8
Primary Ab	[Hematoxylin]	TIGIT	PD-1	CD45	Gzmb	LAG-3	CD103	CD3
Supplier	Dako	Dianova	Abcam	ThermoFisher Invitrogen	Cell Marque	Abcam	Abcam	ThermoFisher Invitrogen
Clone/catalog#	S3301	TG1	NAT105	HI30	EP230	EPR4392	EPR4166(2)	SP7
Dilution	1:50	1:50	1:50	1:100	1:100	1:1000	1:500	1:150
Reaction	1 min	RT, 60 min	RT, 60 min	RT, 30 min	RT, 60 min	RT, 30 min	RT, 30 min	RT, 30 min
Histofine		Anti-mouse	Anti-mouse	Anti-mouse	Anti-rabbit	Anti-rabbit	Anti-rabbit	Anti-rabbit
Reaction		RT, 30 min	RT, 30 min	RT, 30 min	RT, 30 min	RT, 30 min	RT, 30 min	RT, 30 min
AEC reaction time		40 min	40 min	40 min	40 min	20 min	20 min	20 min
	Round 9	Round 10	Round 11	Round 12	Round 13	Round 14	Round 15	Round 16
Primary Ab	CD8	T-bet	FOXP3	Ki-67	TM-3	NKp46	CD39	PanCK
Supplier	Agilent Technologies	Abcam	ThermoFisher eBioscience	Abcam	Cell Signaling Technology	R&D Systems	Abcam	Leica Biosystems
Clone/catalog#	C8/144B	EPR9301	236A/E7	SP6	D5D5R	195314	EPR20267	AE1/AE3
Dilution	1:100	1:100	1:50	1:500	1:100	1:20	1:1000	1:200
Reaction	RT, 30 min	RT, 30 min	RT, 30 min	RT, 30 min	RT, 60 min	RT, 30 min	RT, 30 min	RT, 30 min
Histofine	Anti-mouse	Anti-rabbit	Anti-mouse	Anti-rabbit	Anti-rabbit	Anti-mouse	Anti-rabbit	Anti-mouse
Reaction	RT, 30 min	RT, 30 min	RT, 30 min	RT, 30 min	RT, 30 min	RT, 30 min	RT, 30 min	RT, 30 min
AEC reaction time	20 min	20 min	20 min	20 min	40 min	20 min	20 min	10 min

Panel 2

	Round 1	Round 2	Round 3	Round 4	Round 5	Round 6	Round 7	Round 8	Round 9
Primary Ab	[Hematoxylin]	CD68	CD45	CD80	CD206	CD163	CD33	CD66b	CD73
Supplier	Dako	Abcam	ThermoFisher	R&D Systems	Abcam	Abcam	Abcam	BioLegend	Cell Signaling
Clone/catalog#	S3301	PG-M1	Invitrogen HI30	MAB14037711	Polyclonal	10D6	SP266	G10F5	Technology D7E9A
Dilution	1:50	1:50	1:100	1:25	1:2500	1:100	1:50	1:200	1:50
Reaction	1 min	RT, 60 min	RT, 30 min	RT, 60 min	RT, 30 min	RT, 30 min	RT, 30 min	RT, 30 min	RT, 30 min
Histofine		Anti-mouse	Anti-mouse	Anti-mouse	Anti-rabbit	Anti-mouse	Anti-rabbit	Anti-mouse	Anti-rabbit
Reaction		RT, 30 min	RT, 30 min	RT, 30 min	RT, 30 min	RT, 30 min	RT, 30 min	RT, 30 min	RT, 30 min
AEC reaction time		40 min	40 min	20 min	20 min	20 min	20 min	20 min	20 min
	Round 10	Round 11	Round 12	Round 13	Round 14	Round 15	Round 16	Round 17	
Primary Ab	B7-H3	HLA-DPB1	DC-LAMP	FAP	CD20	PNAd	CD3	PanCK	
Supplier	R&D Systems	Abcam	Merck Millipore	Abcam	Abcam	BioLegend	ThermoFisher Invitrogen	Leica Biosystems	
Clone/catalog#	AF1027	EPR11226	16H11.2	EPR20021	L26	MECA-79	SP7	AE1/AE3	
Dilution	1:40	1:5000	1:200	1:150	1:50	1:100	1:150	1:200	
Reaction	RT, 30 min	RT, 30 min	RT, 30 min	RT, 30 min	RT, 30 min	RT, 30 min	RT, 30 min	RT, 30 min	
Histofine	Anti-goat polyclonal	Anti-rabbit	Anti-mouse	Anti-rabbit	Anti-mouse	Anti-rat	Anti-rabbit	Anti-mouse	
Reaction	RT, 30 min	RT, 30 min	RT, 30 min	RT, 30 min	RT, 30 min	RT, 30 min	RT, 30 min	RT, 30 min	
AEC reaction time	20 min	10 min	30 min	20 min	20 min	20 min	20 min	10 min	

Abbreviations: Ab, antibody; AEC, 3-aminoethyl carbazole; RT, room temperature; TIGIT, T cell immunoreceptor with immunoglobulin and ITIM domains; PD-1, programmed cell death-1; GrzB, granzyme B; LAG-3, lymphocyte activation gene-3; Tbet, T-box expressed in T cells; FOXP3, forkhead box P3; TIM-3, T cell immunoglobulin and mucin domain containing-3; PanCK, pan-cytokeratin; HLA-DPB1, human leukocyte antigen-DPB1; DC-LAMP, dendritic cell-lysosome-associated membrane protein; FAP, fibroblast activation protein; PNAd, peripheral lymph node addressin.

**Supplementary Table S2.** Identification biomarkers for cell lineages.

Panel 1

Lineage	Identification biomarkers
Tumor cell	PanCK <sup>+</sup> CD45 <sup>-</sup>
Leukocyte	PanCK <sup>-</sup> CD45 <sup>+</sup>
T cell	PanCK <sup>-</sup> CD45 <sup>+</sup> CD3 <sup>+</sup>
CD8 <sup>+</sup> T cell	PanCK <sup>-</sup> CD45 <sup>+</sup> CD3 <sup>+</sup> CD8 <sup>+</sup>
Trm-like CD8 <sup>+</sup> T cell	PanCK <sup>-</sup> CD45 <sup>+</sup> CD3 <sup>+</sup> CD8 <sup>+</sup> CD39 <sup>+</sup> CD103 <sup>+</sup>
Regulatory T cell	PanCK <sup>-</sup> CD45 <sup>+</sup> CD3 <sup>+</sup> CD8 <sup>-</sup> FOXP3 <sup>+</sup>
Natural killer cell	PanCK <sup>-</sup> CD45 <sup>+</sup> CD3 <sup>-</sup> NKp46 <sup>+</sup>
T helper 1 cell	PanCK <sup>-</sup> CD45 <sup>+</sup> CD3 <sup>+</sup> CD8 <sup>-</sup> FOXP3 <sup>-</sup> T-bet <sup>+</sup>

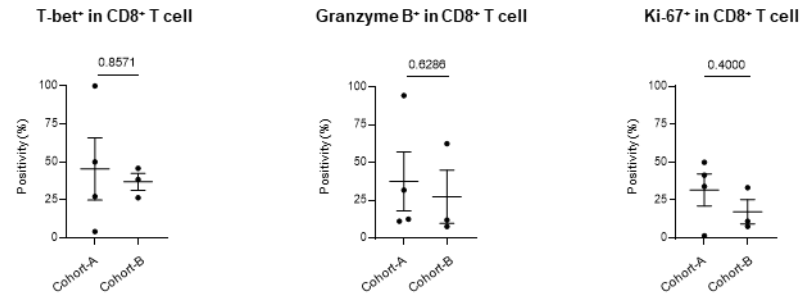
Panel 2

Lineage	Identification biomarkers
Tumor cell	PanCK <sup>+</sup> CD45 <sup>-</sup>
Leukocyte	PanCK <sup>-</sup> CD45 <sup>+</sup>
T cell	PanCK <sup>-</sup> CD45 <sup>+</sup> CD3 <sup>+</sup> CD20 <sup>-</sup>
B cell	PanCK <sup>-</sup> CD45 <sup>+</sup> CD3 <sup>-</sup> CD20 <sup>+</sup>
Myeloid cell	PanCK <sup>-</sup> CD45 <sup>+</sup> CD3 <sup>-</sup> CD20 <sup>-</sup>
Macrophage	PanCK <sup>-</sup> CD45 <sup>+</sup> CD3 <sup>-</sup> CD20 <sup>-</sup> CD68 <sup>+</sup>
M1-macrophage	PanCK <sup>-</sup> CD45 <sup>+</sup> CD3 <sup>-</sup> CD20 <sup>-</sup> CD68 <sup>+</sup> CD163 <sup>-</sup> CD206 <sup>-</sup> CD80 <sup>+</sup>
CD163 <sup>+</sup> M2-macrophage	PanCK <sup>-</sup> CD45 <sup>+</sup> CD3 <sup>-</sup> CD20 <sup>-</sup> CD68 <sup>+</sup> CD163 <sup>+</sup>
CD206 <sup>+</sup> M2-macrophage	PanCK <sup>-</sup> CD45 <sup>+</sup> CD3 <sup>-</sup> CD20 <sup>-</sup> CD68 <sup>+</sup> CD206 <sup>+</sup>
MDSC	PanCK <sup>-</sup> CD45 <sup>+</sup> CD3 <sup>-</sup> CD20 <sup>-</sup> CD33 <sup>+</sup> HLA-DPB1 <sup>-</sup>
PMN-MDSC	PanCK <sup>-</sup> CD45 <sup>+</sup> CD3 <sup>-</sup> CD20 <sup>-</sup> CD33 <sup>+</sup> HLA-DPB1 <sup>-</sup> CD66b <sup>+</sup>
Dendritic cell (DC)	PanCK <sup>-</sup> CD45 <sup>+</sup> CD3 <sup>-</sup> CD20 <sup>-</sup> CD68 <sup>-</sup> HLA-DPB1 <sup>+</sup>
DC-LAMP <sup>+</sup> DC	PanCK <sup>-</sup> CD45 <sup>+</sup> CD3 <sup>-</sup> CD20 <sup>-</sup> CD68 <sup>-</sup> HLA-DPB1 <sup>+</sup> DC-LAMP <sup>+</sup>
CD80 <sup>+</sup> DC	PanCK <sup>-</sup> CD45 <sup>+</sup> CD3 <sup>-</sup> CD20 <sup>-</sup> CD68 <sup>-</sup> HLA-DPB1 <sup>+</sup> CD80 <sup>+</sup>
Fibroblast	PanCK <sup>-</sup> CD45 <sup>-</sup> FAP <sup>+</sup>
Follicular DC	PanCK <sup>-</sup> CD45 <sup>-</sup> PNAd <sup>+</sup>

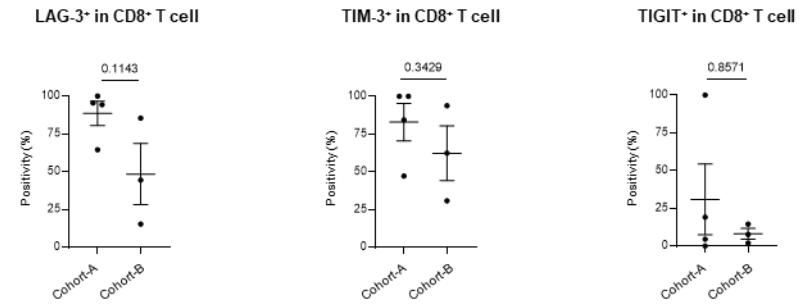
Abbreviations: PanCK, pan-cytokeratin; Trm, tissue-resident memory; FOXP3, forkhead box P3; MDSC, myeloid-derived suppressor cell; HLA-DPB1, human leukocyte antigen–DPB1; PMN, polymorphonuclear; DC-LAMP, dendritic cell–lysosome-associated membrane protein; FAP, fibroblast activation protein; PNAd, peripheral lymph node addressin.

Supplementary Fig. S1

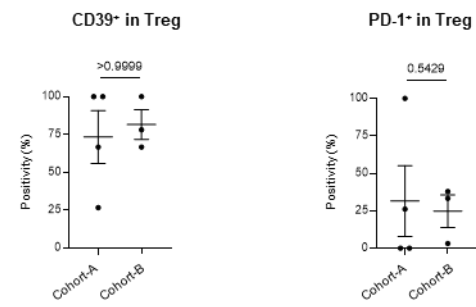
A



B



C

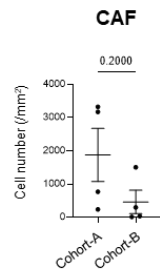




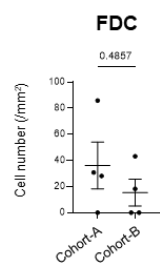
**Supplementary Fig. S1. Multiplex immunohistochemistry–based quantitative single-cell analysis of intratumoral CD8<sup>+</sup> T cells and regulatory T cells (Tregs) expressing specific markers.** (A) Positivity for conventional activated T cell markers in CD8<sup>+</sup> T cells of tumors from cohort-A and cohort-B. (B) Positivity for co-inhibitory molecules in CD8<sup>+</sup> T cells of tumors in cohort-A and cohort-B. (C) Positivity for CD39 and PD-1 in Tregs of tumors from cohort-A and cohort-B. All data indicate the mean  $\pm$  standard error of the mean (SEM). The *P* values for comparisons between the two cohorts were determined with the Mann-Whitney U test. T-bet, T-box expressed in T cells; LAG-3, lymphocyte activation gene–3; TIM-3, T cell immunoglobulin and mucin domain containing–3; TIGIT, T cell immunoreceptor with immunoglobulin and ITIM domains; PD-1, programmed cell death–1.

Supplementary Fig. S2

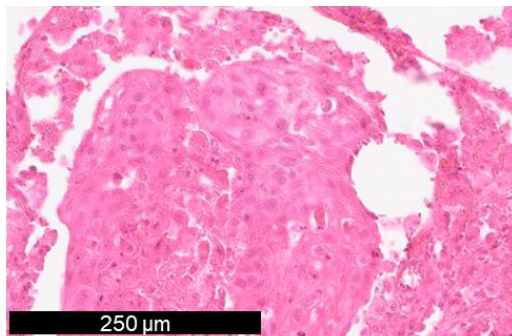
A



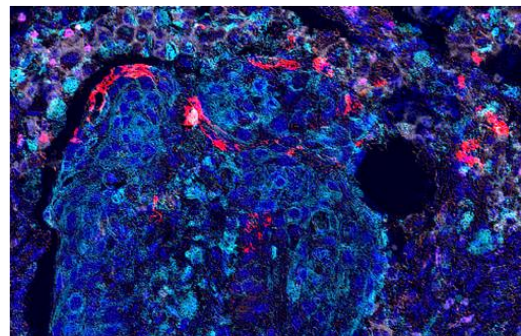
B



HE

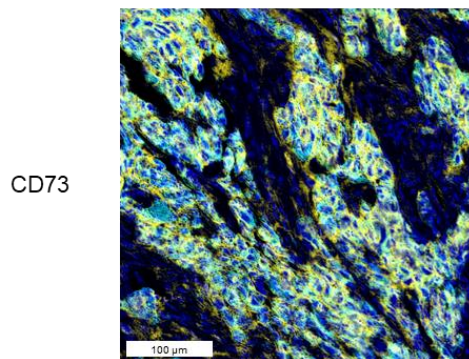


Nucleus CD45 CD20 CD3 FAP PNAAd PanCK

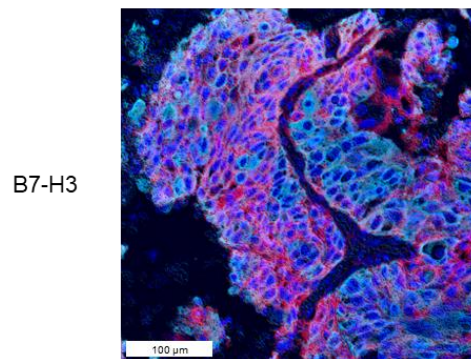


C

Nucleus CD73 PanCK



Nucleus B7-H3 PanCK



**Supplementary Fig. S2. Multiplex immunohistochemistry–based quantitative single-cell analysis of CAFs, FDCs, and tumor cells.** (A) Density of cancer-associated fibroblasts (CAFs, defined as cells positive for fibroblast activation protein [FAP]) in non–tumor cell areas in cohort-A and cohort-B. (B) Density of follicular dendritic cells (FDCs) in non–tumor cell areas in cohort-A and cohort-B. Representative images of the staining pattern for FDCs, including hematoxylin-eosin (HE) staining and a multicolor image showing the nucleus (blue), CD45 (gray), CD20 (yellow), CD3 (pink), FAP (orange), peripheral lymph node addressin (PNAd, red), and pan-cytokeratin (PanCK, cyan), are also presented. Scale bar, 250  $\mu\text{m}$ . Note that solid tertiary lymphoid structures were not detected. Quantitative data in (A) and (B) indicate the mean  $\pm$  standard error of the mean (SEM), and the *P* values for comparisons between the two cohorts were determined with the Mann-Whitney U test. (C) Representative multicolor images of tumor cells expressing CD73 (left) or B7-H3 (right). The images show the nucleus (blue), CD73 (yellow), B7-H3 (red), and PanCK (cyan). Scale bars, 100  $\mu\text{m}$ .